Zoosyst. Evol. 101 (1) 2025, 273–300 | DOI 10.3897/zse.101.143073

PENSOFT

für Naturkunde MUSEUM FÜR NATURKUNDE BERLIN

The millipede genus *Sphaerobelum* Verhoeff, 1924, in Thailand, with descriptions of three new species (Diplopoda, Sphaerotheriida, Zephroniidae)

Khanet Srikampha[1], Thomas Wesener[2], Natdanai Likhitrakarn[3,4], Chirasak Sutcharit[4], Ruttapon Srisonchai[1,4]

1 *Department of Biology, Faculty of Science, Khon Kaen University, Khon Kaen 40002, Thailand*

2 *Zoological Research Museum Alexander Koenig, Leibniz Institute for the Study of Biodiversity Change (LIB), Adenauerallee 160, D-53113 Bonn, Germany*

3 *Program of Agriculture, Faculty of Agricultural Production, Maejo University, Chiang Mai 50290, Thailand*

4 *Animal Systematics Research Unit, Department of Biology, Faculty of Science, Chulalongkorn University, Phayathai Road, Patumwan, Bangkok 10330, Thailand*

https://zoobank.org/32EEBC10-2098-48B5-888F-2429C1A6A326

Corresponding author: Ruttapon Srisonchai (ruttasr@kku.ac.th)

Academic editor: Luiz Felipe Iniesta ♦ **Received** 1 December 2024 ♦ **Accepted** 18 January 2025 ♦ **Published** 13 February 2025

Abstract

Three new species of the giant pill-millipede genus *Sphaerobelum* Verhoeff, 1924, from Thailand and Laos, are described based on an integrative approach that combines morphological characters and COI data; these are *S. nonghinensis* Srikampha & Srisonchai, **sp. nov.**, *S. onyx* Srikampha & Srisonchai, **sp. nov.**, and *S. petramurum* Srikampha & Srisonchai, **sp. nov.** Additionally, new material of previously described species, *S. aesculus* Rosenmejer & Wesener, 2021, *S. truncatum* Wongthamwanich, 2012, and *S. turcosa* Srisonchai & Pimvichai, 2023, were collected and examined. The new species can be distinguished from all congeners by a combination of unique characters, including body colour, endotergum, vulva, and details of the telopods. The validity of these new species is further supported by high genetic distances from their congeners in the 658 base pairs of the COI barcoding fragment, ranging from 13.24–30.12%. Preliminary phylogenetic analyses using Bayesian inference and maximum likelihood indicate that each new species forms a distinct clade, supporting their morphological uniqueness, though the interrelationships with most other congeners remain unsupported. All new species are restricted to narrow distribution areas in Thailand and Laos, suggesting they are endemic to these regions. Morphological characters of the new species are illustrated, and an identification key and a distribution map for known *Sphaerobelum* species in Thailand are also provided.

Key Words

Biodiversity, endemism, limestone, phylogeny, systematics

Introduction

Giant pill millipedes in the family Zephroniidae (order Sphaerotheriida) are remarkable not only for their ability to roll into a ball and their larger size but also for their considerable diversity. They have a long evolutionary history shaped by past geological events (Wesener and VandenSpiegel 2009; Wesener et al. 2010), and their distribution spans regions including the Seychelles, Nepal and northern India, Southeast Asia, and Southeast China (Wesener 2016). This wide geographic range highlights the adaptability and the ecological significance of these unique creatures.

In Thailand, three genera of Zephroniidae have hitherto been reported: *Zephronia* Gray, 1832; *Prionobelum* Verhoeff, 1924; and *Sphaerobelum* Verhoeff, 1924. The genus *Zephronia* includes 14 species in the country,

Copyright *Srikampha, K. et al.* This is an open access article distributed under the terms of the Creative Commons Attribution License (CC BY 4.0), which permits unrestricted use, distribution, and reproduction in any medium, provided the original author and source are credited.

while *Sphaerobelum* and *Prionobelum* contain four and two species, respectively. While research on *Zephronia* is actively progressing, the systematic frameworks for the *Sphaerobelum* and *Prionobelum* seem to be in the early stages (Wesener 2016, 2019). This indicates a need for further studies to enhance our understanding of these lesser-explored genera within the Zephroniidae.

Currently, *Sphaerobelum* comprises 24 (with all but 5 described in the last six years) described species inhabiting southern China through mainland Southeast Asia (Wongthamwanich et al. 2012; Wesener 2016, 2019; Semenyuk et al. 2018, 2020; Zhao et al. 2020, 2022; Rosenmejer et al. 2021; Bhansali and Wesener 2022; Srisonchai et al. 2023). The four species of the genus in Thailand are *S. aesculus* Rosenmejer & Wesener, 2021, *S. meridionalis* Bhansali & Wesener, 2022, *S. truncatum* Wongthamwanich, 2012, and *S. turcosa* Srisonchai & Pimvichai, 2023. Although initial research on Thai *Sphaerobelum* began in 2012 (Wongthamwanich et al. 2012) and continued recently in 2022 and 2023, there remains limited information regarding their phylogenetic relationships.

The northeast of Thailand features a diverse landscape that encompasses various types of topological habitats, such as limestone, sandstone, and granite (Joint Publication Research Service 1965; Furukawa and Pichai 1989; Prueksapong et al. 2015). Such an ecological variety positions the area as an important biodiversity hotspot within the country. Known for its rich biological diversity, the region is particularly vibrant along several mountain ranges and major river basins, which support a wide range of invertebrates (Clements et al. 2006, 2008; Plant 2014; Pholyotha et al. 2020), including the giant pill millipedes (Likhitrakarn et al. 2023).

Intensive field surveys conducted in both karstic and non-karstic habitats of northeastern Thailand within the Mekong River Basin from 2020 to 2024 have resulted in a small collection of both described and undescribed *Sphaerobelum* species. A thorough examination of general external features led to the confirmation of three distinct morphotypes. In this study, we present the descriptions of three new species of giant pill millipedes currently classified in the genus *Sphaerobelum* based on comparative morphological and COI barcoding data, with notes on newly collected materials of the described species from Thailand.

Materials and methods

Specimen collections

This research was conducted with the approval of the Animal Care and Use Committee at Khon Kaen University (protocol no. IACUC-KKU-71/67) and with permission to conduct research in protected areas (Department of National Parks, Wildlife, and Plant Conservation; protocols no. 23103 and 23104). Specimens were collected by hand during the daytime in northeastern Thailand from 2020 to 2024, and photographs of living specimens were taken using a Canon 90D digital camera equipped with a Canon EF 100 mm f/2.8 Macro USM lens. All specimens were euthanised in accordance with the AVMA guidelines for the euthanasia of animals (American Veterinary Medical Association 2020) and were preserved in 70% ethanol for morphological studies and in 95% ethanol for DNA sequence analysis. The distribution map of all *Sphaerobelum* species in Thailand was prepared using the online map from Elastic Terrain Map (Willett et al. 2015) and adjusted with Adobe Photoshop 2022.

Morphological study

The morphological terms used in the descriptions followed Wongthamwanich et al. (2012), Wesener (2019), Bhansali and Wesener (2022), and Srisonchai et al. (2023, 2024b).

We examined 156 specimens under a stereo microscope. Body parts for scanning electron microscopy (SEM) were dissected, mounted on stubs, air-dried in a dry cabinet for 24 hours, and then coated with gold. SEM photographs were taken under a high vacuum in JEOL, JSM-5410 LV at the Faculty of Science, Khon Kaen University. All photographs and SEM images were processed and adjusted in Adobe Photoshop 2022.

Some available type materials of *S. aesculus* (NHMD 621693), *S. bicorne* Attems, 1938 (NHM 2196), *S. clavigerum* Verhoeff, 1924 (ZMB), *S. separatum* Attems, 1953 (NHMW 2227), and *S. turcosa* (CUMZ) were morphologically examined and compared with the new species.

Morphological abbreviations

3it 3-combed inner tooth of mandible,
bu bursa of vulva,
co condyles of mandible,
cp cuticular impression of endotergum,
Cp central pad of gnathochilarium,
ct central tooth,
cx coxa,
et external tooth of epipharynx,
Et external tooth of mandibular gnathal lobe,
fe femur,
ia inner area of endotergum,
Ia inner area of mandible,
imf immovable finger of telopod,
ip inner palpi of gnathochilarium,
ll lamellae lingulales of gnathochilarium,
ma middle area of endotergum,
me mentum,
ml membranous lobe of telopod,
mp molar plate of mandible,
op operculum of vulva,
pl pectinate lamellae of mandible,
pm posterior margin of endotergum,
po postfemur,

pre prefemur,
rsp row of spine on epipharynx,
sc sensory cone,
Sp apico-mesal spine of leg (tooth),
sp spine on telopoditomere 4 of posterior telopod,
st stipites,
st-pl stigmatic plate,
ta tarsus,
ti tibia.

Institutional abbreviations

CUMZ Museum of Zoology, Chulalongkorn University, Thailand;
MZKKU Khon Kaen University Museum of Zoology, Thailand;
NHM Natural History Museum, England;
NHMD Natural History Museum of Denmark, Denmark;
NHMW Naturhistorisches Museum Wien, Vienna, Austria;
ZMB Zoologisches Museum Berlin, Germany;
ZFMK Zoological Research Museum Koenig, Bonn, Germany.

Phylogenetic analysis

A total of 13 genomic DNA samples were extracted from legs using the NucleoSpin Tissue kit, following the manufacturer's extraction protocol. Fragments of mitochondrial cytochrome c oxidase subunit 1 (COI) were amplified using the HCO-2198/LCO-1490 primers (Folmer et al. 1994) as outlined in the protocol (Pimvichai et al. 2020; Srisonchai et al. 2024b). The PCR products were completely sequenced in both forward and reverse directions by an automated sequencer at Bioneers Co. (Korea). All new sequences obtained in this study were uploaded to GenBank with accession numbers PQ838982–PQ838994 (Suppl. material 1).

The sequences were aligned into an appropriate reading frame in MEGA 11 (Tamura et al. 2021) to inspect for missing sites and stop codons. All 97 sequences were analysed, including 13 new sequences and 84 sequences available from GenBank. The outgroups were selected based on the recent studies by Bhansali and Wesener (2022) and Srisonchai et al. (2024b), which included *Zephronia* spp., *Cryxus ovalis* (Linnaeus, 1758), *Prionobelum* spp., *Epicyliosoma* sp., *Arthrosphaera brandtii* (Humbert, 1865), *Sphaeromimus splendidus* Wesener & Sierwald, 2005, and *Glomeris marginata* (Villers, 1789).

The phylogenetic trees were reconstructed using online computational analyses from the CIPRES Science Gateways (Miller et al. 2010) under two approaches: maximum likelihood (ML) and Bayesian inference (BI). The ML tree was reconstructed in IQ-tree on XSEDE 1.6.6 with 10,000 bootstrap replicates (Minh et al. 2020) and the best fit model generated by ModelFinder (TIM2+F+I+G4) (Kalyaanamoorthy et al. 2017). For BI, the preparation of the input file was performed in KAKUSAN 4.0 (Tanabe 2011). BI tree was performed in MrBayes on XSEDE 3.2.7a (Ronquist et al. 2012) with four Markov Chain Monte Carlo algorithms (MCMC), running for 50 million generations, sampling every 1,000 generations. Both ML and BI trees were processed using FigTree v. 1.4.4 (Rambaut 2018) and subsequently adjusted in Adobe Illustrator 2023. A clade from the obtained phylogenetic trees was evaluated for node robustness, defined as strong support when the bootstrap support values (BS) for maximum likelihood (ML) exceed 70% and the posterior probability (PP) for Bayesian Inference (BI) exceeds 0.95 (Huelsenbeck and Hillis 1993; Larget and Simon 1999).

The intergeneric, interspecific, and intraspecific genetic distances were also estimated as uncorrected *p*-distance under the pairwise parameter in MEGA 11.

Results

Genetic analyses

The sequences of the COI gene fragment comprised 658 base pairs, and the sequence annotation contained 370 variable sites, 287 conservative sites, and 310 sites that were parsimony informative. The genetic distances between related outgroups (*Arthrosphaera brandtii* + *Epicyliosoma* sp. + *Glomeris marginata* + *Sphaeromimus splendidus*) and *Sphaerobelum* + *Zephronia* + *Prionobelum* + *Cryxus* were 20.6–32.5%. The intergeneric distances for *Sphaerobelum* and *Zephronia* were 6.8–25.2%, 17.4–23.0% for *Sphaerobelum* and *Prionobelum*, and 18.5–24.2% for *Sphaerobelum* and *Cryxus*. The interspecific distances within *Sphaerobelum*, *Zephronia*, and *Prionobelum* ranged from 10.2–24.6%, 17.4–18.4%, and 9.2–24.2%, respectively. The intraspecific distances of *S. nonghinensis* sp. nov., *S. onyx* sp. nov., and *S. petramurum* sp. nov. ranged from 0–0.3%, 0–5.0%, and 0–7.2%, respectively. All three new species were distinguished from one another by an interspecific *p*-distance ranging from 13.2% to 22.1%. Details of the genetic distances are provided in Suppl. material 2.

The phylogenetic trees generated using Bayesian inference (BI) and maximum likelihood (ML) methods resulted in different topologies, particularly in the deep and internal nodes (Fig. 1). In the BI tree, members of *Sphaerobelum* were interspersed with the genera *Zephronia*, *Prionobelum*, and *Cryxus*, forming four major clades in a polytomy. In contrast, the ML tree depicted a polyphyletic group of *Sphaerobelum* in three major clades. Both trees exhibited low support values. These results indicate unresolved relationships and raise significant questions about the monophyly of these genera in their current taxonomic status.

Although the overall phylogenetic tree remains unresolved, this study effectively highlights the positioning of

the three new species alongside their closely related congeners. Both BI and ML trees clearly show the three new species recovered as monophyletic with high support (PP = 1.0, BS = 91), with the clades formed by *S. laoticum* Wesener, 2019, and *S. schwendingeri* Wesener, 2019, as a sister group (PP = 1.0, BS = 92), supporting their similarity in morphological characters.

S. nonghinensis sp. nov. occupies the first lineage to diverge among the other two new species. In contrast, *S. onyx* sp. nov. and *S. petramurum* sp. nov. are clustered together.

Systematics

Class Diplopoda de Blainville in Gervais, 1844
Order Sphaerotheriida Brandt, 1833
Family Zephroniidae Gray, 1843
Subfamily Zephroniinae Gray, 1843
Tribe Zephroniini Gray, 1843

Genus *Sphaerobelum* Verhoeff, 1924

Type species. *Sphaerobelum clavigerum* Verhoeff, 1924, by subsequent designation of Jeekel (1971: 28).

Other species included. 26 species (plus three described below: Verhoeff 1924; Attems 1938, 1953; Wongthamwanich et al. 2012; Semenyuk et al. 2018, 2020; Wesener 2019; Zhao et al. 2020, 2022; Rosenmejer et al. 2021; Bhansali and Wesener 2022; Srisonchai et al. 2023).

Distribution. China (3 species), Laos (10 species), Thailand (7 species), and Vietnam (7 species).

Diagnosis. A genus of Zephroniinae in which the posterior telopod has 4 telopoditomeres distal to the syncoxite, immovable finger apically uniquely enlarged and massively swollen (except for *S. aesculus*, *S. meridionalis*, and *S. benqii*, in which there is just a swollen spot). Anterior telopod either with 3 or 4 podomeres distal to syncoxite, with podomeres 3 and 4 simple, either completely fused, partly fused, or completely separated.

See more detail of diagnosis in Wongthamwanich et al. (2012), Wesener (2016), Semenyuk et al. (2018), and Srisonchai et al. (2024b).

Remarks. Wesener (2019) divided the genus into two main groups based on the modification of the mesal margin of the leg femur. The first group consists of species with either a flat margin or inconspicuous tiny teeth (hardly visible under a stereomicroscope); here, we refer to this as the 'unmodified femur.' The second group, the 'modified femur,' includes species with conspicuous teeth along the margin (easily visible under a normal stereomicroscope).

In Thailand, four previously recorded species (*S. aesculus*, *S. meridionalis*, *S. truncatum*, and *S. turcosa*), as well as the three new species described here, are assigned into the 'unmodified femur' group, characterised by no or only inconspicuous teeth on the femur of the leg.

Sphaerobelum aesculus Rosenmejer & Wesener, 2021

Figs 15A, B, 16

Sphaerobelum aesculus Rosenmejer & Wesener, 2021 in Rosenmejer et al. 2021: 114.

Sphaerobelum aesculus—Likhitrakarn et al. 2023: 55; Srisonchai et al. 2023: 52.

New material examined: Thailand • ♀ (MZKKU), Nakhon Si Thammarat Province, Lan Saka District, Khao Kaeo Subdistrict, Kaeo Surakan Cave, 60 m a.s.l., 8°21'40.3"N, 99°47'07.4"E, 17 May 2023, K. Srikampha & R. Srisonchai coll. • 2 ♂♂ (MZKKU), Surat Thani Province, Phanom District, Mae Yai Waterfall, 400 m a.s.l., 8°53'18.0"N, 98°29'58.9"E, 10 July 2017, R. Srisonchai & C. Sutcharit coll. • ♂ (MZKKU), Surat Thani Province, Phanom District, Waterfall in Khao Sok National Park, 6 May 2017, R. Srisonchai & C. Sutcharit coll. • ♂, ♀ (MZKKU), Surat Thani Province, Wiang Sa District, Khiri Rat Pattana Temple (Wat Khao Poon), 68 m a.s.l., 8°31'37"N, 99°22'59"E, 4 July 2017, R. Srisonchai & C. Sutcharit coll.

Distribution. This species is currently known from the limestone areas in Krabi, Nakhon Si Thammarat, Phuket, and Surat Thani Provinces.

Remarks. No morphological variation has been observed in the examined specimens, while the intraspecific genetic distance based on the 658 base pairs COI fragment ranges to 6.1%.

Sphaerobelum meridionalis Bhansali & Wesener, 2022

Fig. 15C, D

Sphaerobelum meridionalis Bhansali & Wesener, 2022: 364.

Sphaerobelum meridionalis—Likhitrakarn et al. 2023: 55; Srisonchai et al. 2023: 52.

Distribution. This species is known only from the type locality in Yala Province.

Sphaerobelum nonghinensis Srikampha & Srisonchai, sp. nov.

https://zoobank.org/C638CEF4-6641-45E4-9472-B46874557100

Figs 2–5, 14A, B, 15E, F, 16

Type material. ***Holotype.*** Thailand • ♂ (MZKKU-MYR0001), Loei Province, Nong Hin District, Suan Hin Pha Ngam (Hin Pha Ngam Park), 17°03'02"N, 101°44'40"E, ca. 680 m a.s.l., 23 October 2021, K. Srikampha and N. Srimongkol coll. ***Paratypes.*** Thailand • 17 ♂♂, 12 ♀♀ (MZKKU-MYR0002), 2 ♂♂, ♀ for SEM (MZKKU-MYR0002), same data as holotype. • 4 ♂♂, 9 ♀♀ (MZKKU-MYR0002), same data as holotype, 27 September 2024, K. Srikampha coll. • ♂, ♀ (CUMZ-MYR0031), same data as holotype. • ♂, ♀ (NHM), same data as holotype. • ♂, ♀ (NHMD), same data as holotype. • ♂, ♀ (NHMW), same data as holotype. • ♂, ♀ (ZFMK), same data as holotype.

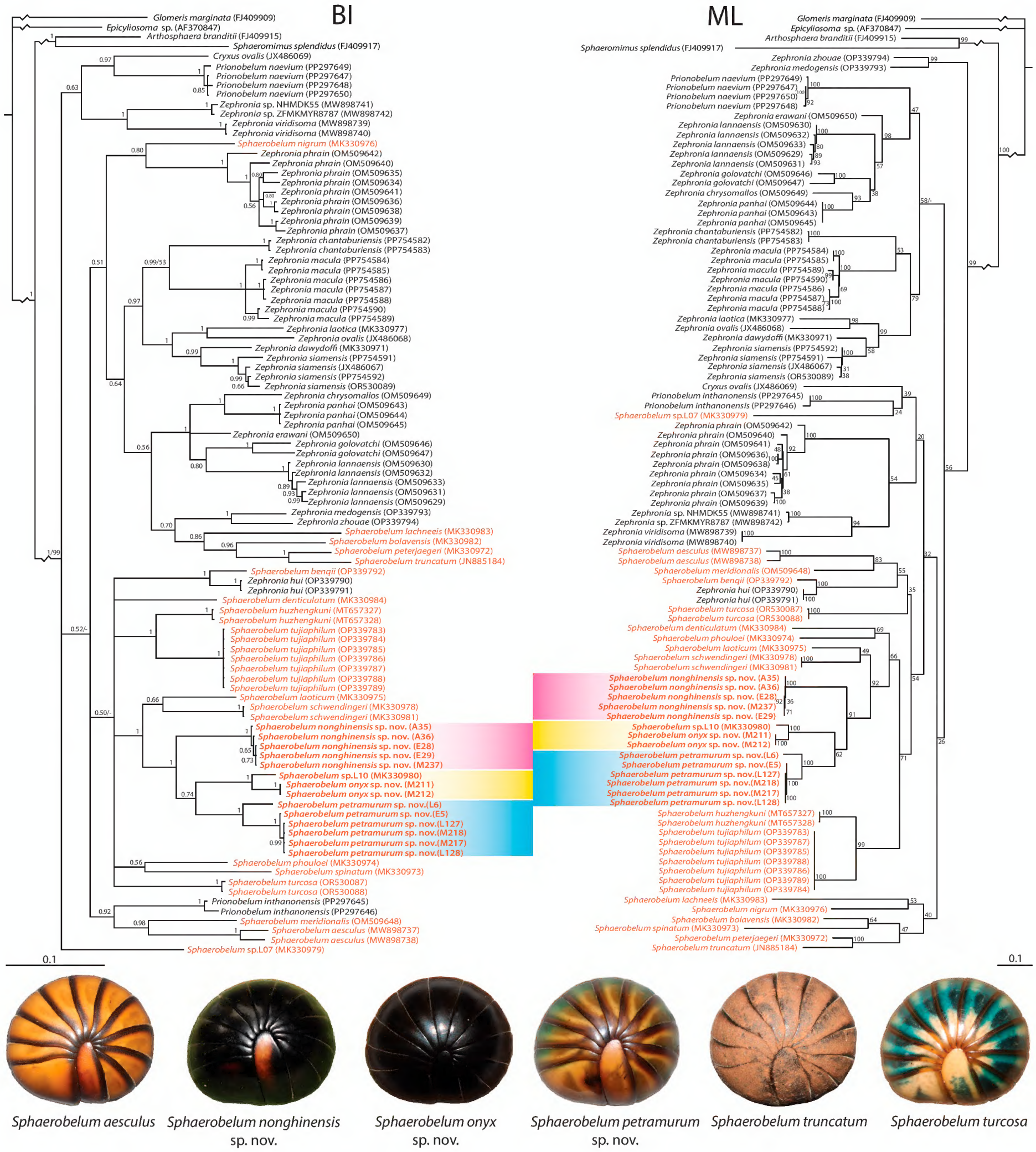

Figure 1. Bayesian inference (BI) and maximum likelihood (ML) trees of genus *Sphaerobelum*. Numbers on nodes represent posterior probabilities (PP) from BI and bootstrap support (BS) from ML. Colours on the background indicate the three new species, relating to the photograph of live specimens. The scale bar represents the branch length.

Additional material examined—non-type. THAILAND • ♀ (MZKKU), Loei Province, Nong Hin District, Wat Tham Pha Fai, 17°02'37"N, 101°44'10"E, ca. 718 m a.s.l., 12 September 2021, K. Srikampha coll. • ♂ (MZKKU), Loei Province, Nong Hin District, Wat Tham Sung (Wat Tham Pha Nang Khoi), 17°04'31"N, 101°47'08"E, ca. 344 m a.s.l., 12 September 2021, K. Srikampha coll.

Diagnosis. *S. nonghinensis* sp. nov. differs in the femur of the legs, in which only the apical margin carries a few teeth, a character only shared with *S. bicorne* Attems, 1938, *S. bolavensis* Wesener, 2019, as well as *S. onyx* sp. nov. and *S. petramurum* sp. nov. described below. *S. nonghinensis* sp. nov. differs from both *S. bicorne* and *S. bolavensis* in the presence of a "hook" on telopoditomere 4 of the posterior telopods. Differs in the unique colouration pattern, black, with orange markings only on the thoracic shield and anal shield from other known *Sphaerobelum* species, e.g., from *S. petramurum* sp. nov., which is greenish-bluish brown, and from *S. onyx* sp. nov., which is entirely black. *S. nonghinensis* sp. nov. has a "hook" on telopoditomere

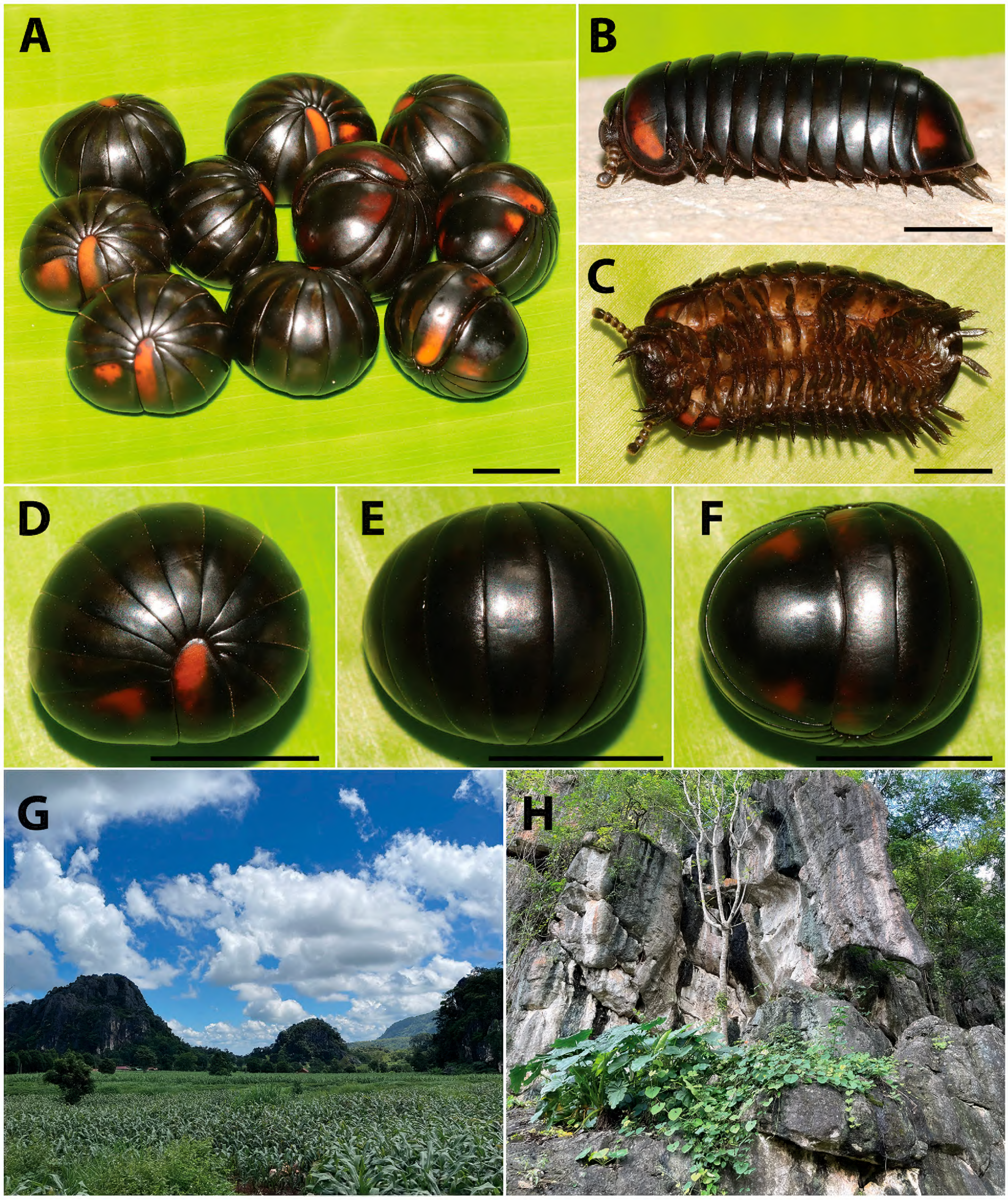

Figure 2. Photograph of live specimens of *Sphaerobelum nonghinensis* sp. nov. **A–F.** Paratypes (MZKKU-MYR0002); **G, H.** Habitat at the type locality (limestone). Scale bars: 10.0 mm.

4 of the posterior telopods that resembles those of *S. clavigerum*, *S. hirsutum*, *S. laoticum*, *S. onyx* sp. nov., *S. petramurum* sp. nov., *S. schwendingeri*, *S. separatum*, and *S. splendidum*. The new species differs from *S. clavigerum* in the presence of a single short or dot-like locking carina on the anal shield (vs. 3× long), from *S. hirsutum* and *S. separatum* in the presence of glabrous tergites (vs. hairy). It differs from *S. laoticum* and *S. schwendingeri* by having < 60 apical cones on antenna (vs. 81–86 in *S. laoticum*, 36–73 in *S. schwendingeri*) and by having a greenish-brown antenna (vs. red). It differs from *S. splendidum* by having an elongated telopoditomere 2 of the anterior telopod (vs. short, as long as telopoditomere 3).

Description. ***Measurements*:** Male holotype; body length 26.1 mm; width (broadest) of thoracic shield 13.0 mm, of tergite 7 = 13.1 mm; height of tergite 7 = 7.7 mm.

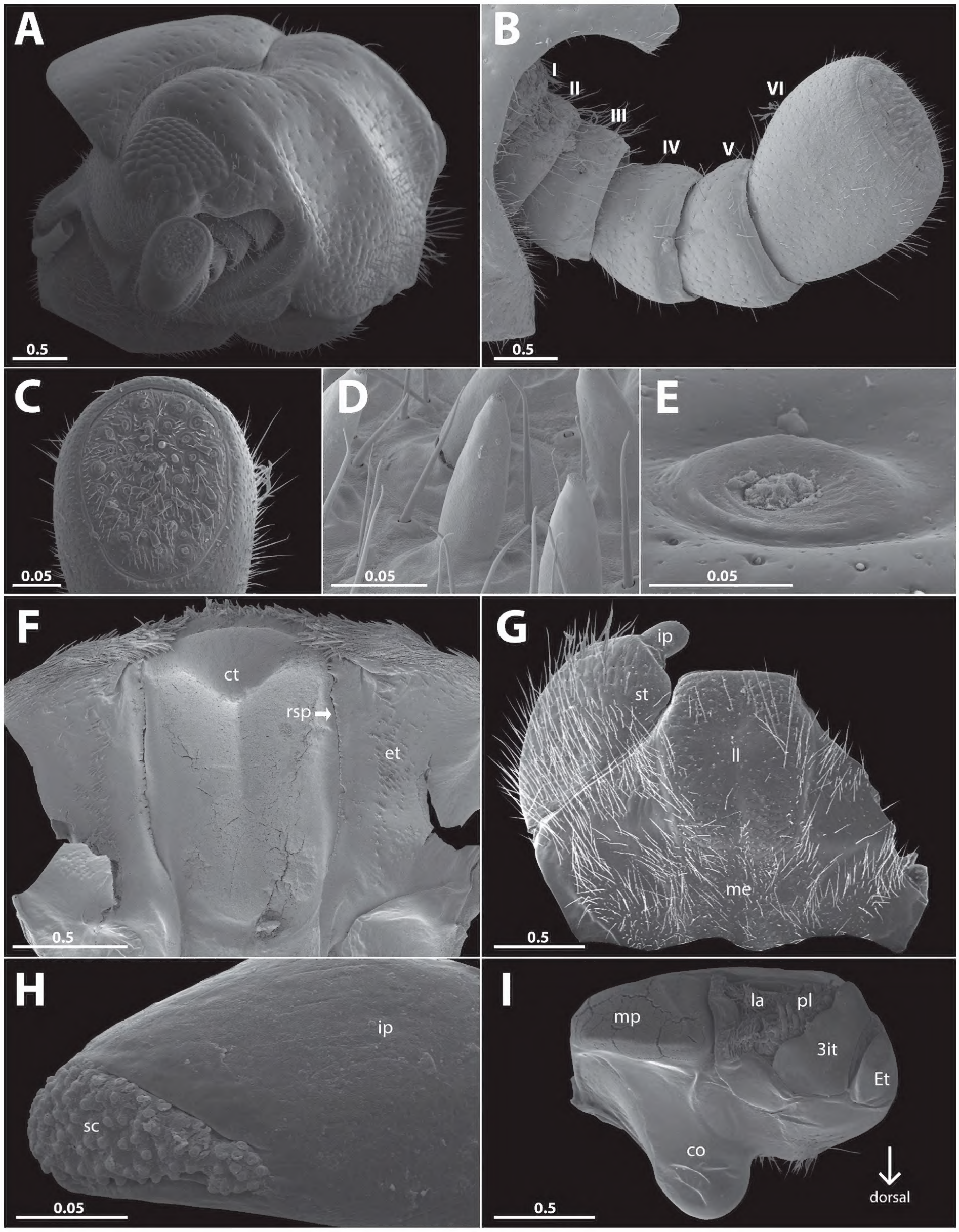

Figure 3. SEM of *Sphaerobelum nonghinensis* sp. nov., ♂ paratype (MZKKU-MYR0002). **A.** Head region, lateral view; **B.** Left antenna, anterior view; **C.** Antennal disc, anterior view; **D.** Apical cones on antennal disc, lateral view; **E.** Organ of Tömösváry, lateral view; **F.** Epipharynx, ventral view; **G.** Gnathochilarium, ventral view; **H.** Sensory cones on inner palpi, anterior view; **I.** Mandible, mesal view. Abbreviations: 3it = 3-combed inner tooth, co = condylus, ct = central tooth, et = external tooth, Et = external tooth, Ia = inner area, ip = inner palpi, ll = lamellae linguales, me = mentum, mp = molar plate, pl = pectinate lamellae, rsp = row of spines, sc = sensory cone, st = stipite. Scale bars in millimetres.

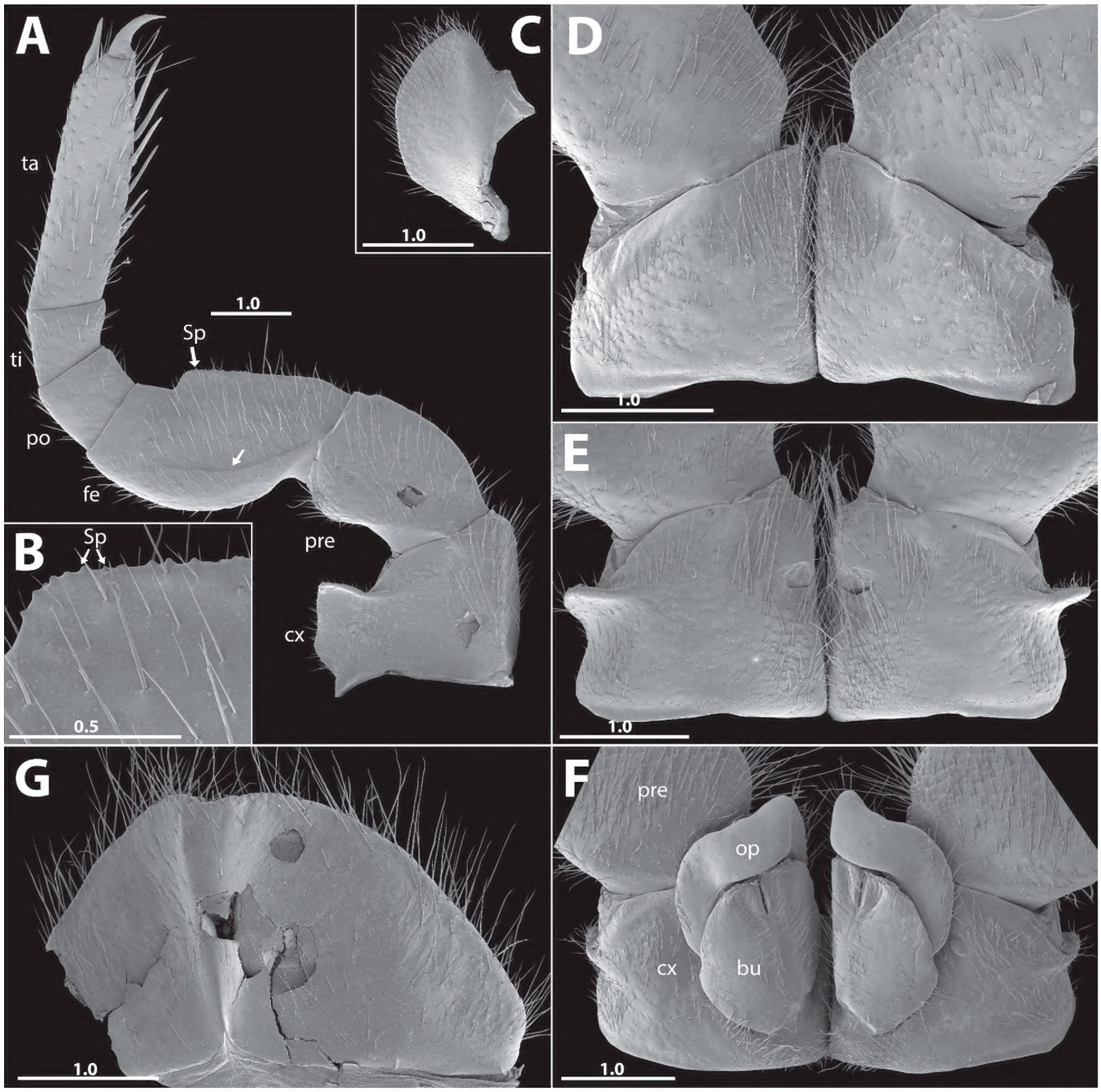

Figure 4. SEM of *Sphaerobelum nonghinensis* sp. nov. **A–E.** ♂ paratype (MZKKU-MYR0002); **F, G.** ♀ paratype (MZKKU-MYR0002). **A.** Leg 11, arrow points to femoral ridge; **B.** Small spines on femur; **C.** Stigmatic plate 1; **D.** Coxae of legs 1; **E.** Coxae of legs 2 with gonopores; **F.** Leg 2 with vulvae; **G.** Subanal plate. Abbreviation: bu = bursa, cx = coxa, fe = femur, op = operculum, po = postfemur, pre = prefemur, Sp = apico-mesally spine of leg, ta = tarsus, ti = tibia. Scale bars in millimetres.

Males: body length = 24.4–27.9 mm; width (broadest) of thoracic shield = 11.8–12.5 mm, of tergite 7 = 12.2–13.1 mm; height of tergite 7 = 7.9–8.0 mm. Females: body length = 25.7–28.7 mm; width (broadest) of thoracic shield = 13.1–14.6 mm, of tergite 7 = 14.0–15.7 mm; height of tergite 7 = 8.4–10.1 mm.

Colouration (Fig. 2A–F): Live specimens with dark body colour, shiny. Head, collum, and tergites shiny black. Lateral margins of both thoracic and anal shields contrastingly orangish brown. Antennae brown. Legs and venter greenish brown. Specimens in 70% alcohol after 4 years changed to brownish black.

Head (Fig. 3A, E): Trapeziform, sparsely setose; setae on anterior part longer than posterior one; each seta located inside small pit. With 75–87 ommatidia (ocelli) in males and 72–78 in females. Aberrant ommatidium present at brim of antennal groove. Organ of Tömösváry situated at brim near ocelli, separated from eye field. No sclerotised crest/ridge between antennal socket and eye field.

Antennae (Figs 2B, C, 3A–D): Short and stout, covered by long and dense setae; last antennomere reaching back to leg pair 2 or 3. Lengths of antennomeres 6>5=4>3>2=1. Antennomere 6 apically rounded, oval; with sensilla basiconica apically. Apical disc flat, with 14–50 apical cones in male or 29–34 in female.

Epipharynx (Fig. 3F): With a regular central tooth (ct); laterally with numerous external teeth (et), short; inner area of each side with a row of crenate spines (rsp).

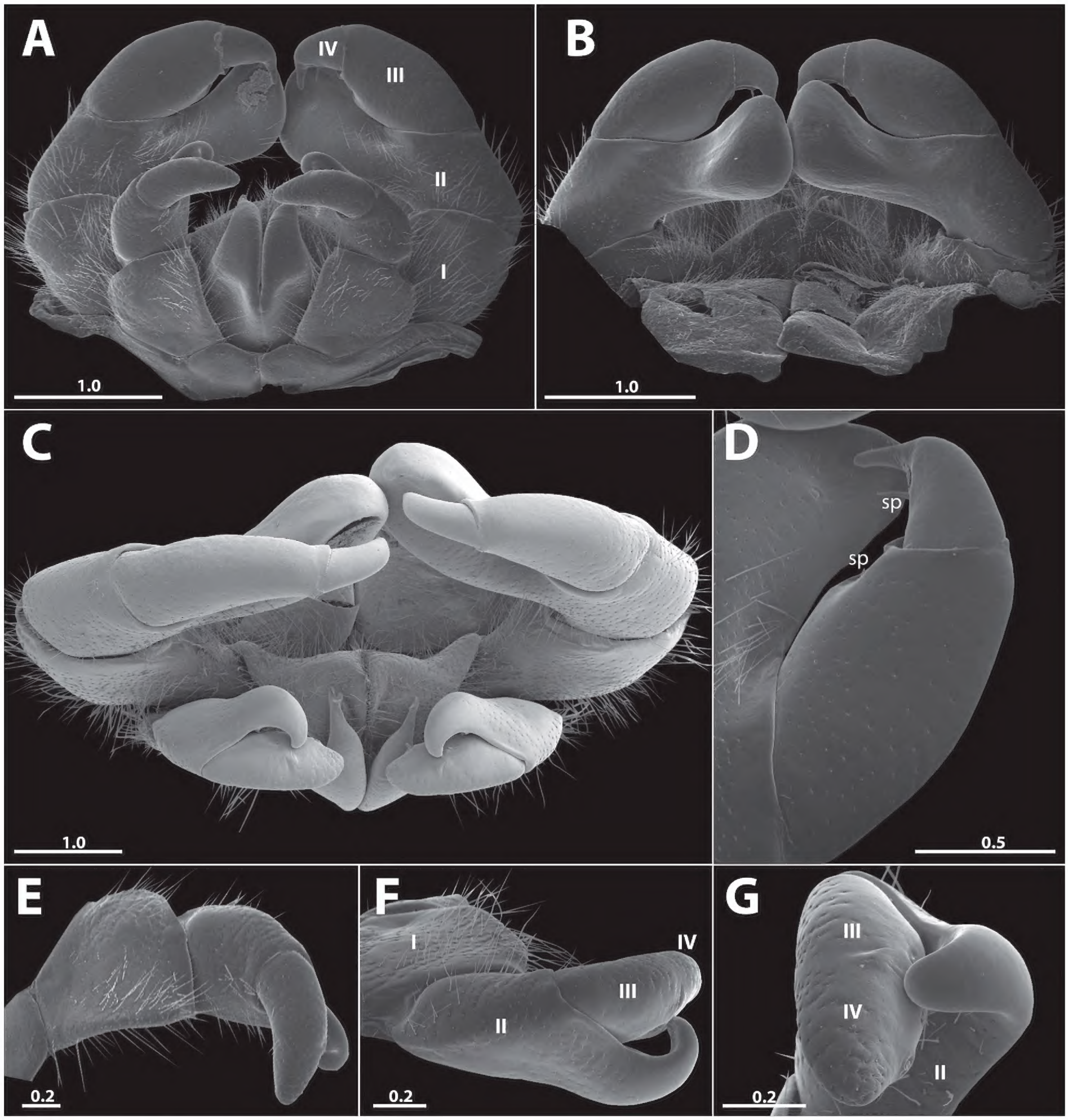

Figure 5. SEM of *Sphaerobelum nonghinensis* sp. nov., ♂ paratype (MZKKU-MYR0002). **A–C.** Telopods, anterior, posterior, and ventral views, respectively; **D.** Right posterior telopod, anterior view; **E–G.** Anterior telopod, anterior, sublateral, and subventral views, respectively. Abbreviations: sp = telopoditomere 4 of posterior telopod's spine. Scale bars in millimetres.

Gnathochilarium (Fig. 3G, H): With long and dense setae. Lamellae linguales (ll) rectangular, flat apically. Central pads (Cp) modified, with numerous sensory cones. Stipites (st) large; located laterally to lamellae linguales. Mentum (me) large, fused. Lateral palpi inconspicuous. Inner palpi (ip) with sensory cones (sc) arranged in two fields.

***Mandibles* (gnathal lobe)** (Fig. 3I): With undivided external tooth (Et) and with conspicuous 3-combed inner tooth (3it). With 4–5 rows of pectinate lamellae (pl). Inner area (Ia) with group of tiny teeth. Molar plate (mp) flat, velvet-like; lacking a membranous fringe. Condylus (co) conspicuous, apically with two distinct ridges.

Tegument (Fig. 2A–F): Shiny; collum, thoracic shield, tergites, and anal shield sparsely microscopic setose; each seta located in an inconspicuous pit. Anterior margins of midbody tergite and anal shield with a few rows of long setae.

Collum (Figs 2B, 3A): Subsemicircular; tip of lateral margin obtuse.

***Thoracic shield*:** Anteriorly with shallow and large grooves separated by a long ridge. Groove and ridge smooth, without setae. Sloped towards groove laterally with 4 inconspicuous keels.

***Midbody tergite*:** With a row of oval impressions at anterior margin. Tips of midbody paratergites projecting posteroventrad.

***Paratergites*:** Paratergites 3 and 4 slender, slightly attenuate; tip sharp. Paratergites 5–12 wide; tip obtuse.

***Anal shield*:** Large and well-rounded in female, slenderer in male. Underside with a single, short, black locking carina, as long as those of tergites, sometimes dotlike.

Endotergum of midbody tergite (Fig. 14A, B): Posterior margin (pm) flat, regular. Outer area (oa) wide; without setae. Marginal bristles arranged in 3–4 rows; tips of the longest bristles not protruding above posterior margin. Middle area (ma) with a single row of conspicuous, circular cuticular impressions (cp); distance between impressions twice as long as individual diameter. Inner area (ia) without tubercles or setae.

***Pleurites* (laterotergites):** First pleurite slender, boomeranglike; apical margin attenuated, strongly projecting into a wide tip. Pleurite 2 wider than the first one, projecting into obtuse tip. All remaining pleurites flat and broad, apical margin slightly extended.

Subanal plate (Fig. 4G): Densely setose; large and wide; well-rounded; apical margin slightly concave.

Stigmatic plates (Fig. 4C): First stigmatic plate slender, apex well-rounded. Second stigmatic plate in both sexes not curved.

Legs (Fig. 4A–F): All podomeres sparsely setose. Coxa (cx) large; coxal process absent in first legs; legs 2–21 laterally with conspicuous coxal ridge (legs 2 of female slightly smaller than in male). Prefemur (pre) short; apico-mesally with inconspicuous projection. Femur (fe) 1.5 times longer than wide, with long femoral ridge in all leg pairs; apico-mesally with dentate margin, carrying inconspicuous teeth (Sp). Postfemur (po) and tibia (ti) short. Tarsus (ta) of midbody legs quite long, 3.4 times longer than wide, as long as length of femur+postfemur. First two leg pairs without apical spine; leg-pair 1 with 2 ventral spines; leg-pair 2 with 5 ventral spines; leg-pair 3 with 5 or 6 ventral spines and 1 apical spine; leg pairs 4–21 with 6 or 7 ventral spines and 1 apical spine. Claw normal, with a small notch at base.

Male gonopore (Fig. 4E): Small, triangular; covered by long setae.

Anterior telopods (Fig. 5A, C, E–G): First telopoditomere large, stout, apically widening. Telopoditomere 2 large, with projection as long as telopoditomere 3. Immovable finger (process of telopoditomere 2) short; clearly seen in posterior and ventral views; almost as long as telopoditomere 3; strongly curved; attenuate near tip; tip obtuse. Telopoditomere 3 indistinctly demarcated from telopoditomere 4 (with inconspicuous suture), both of equal length and cylindrical; telopoditomere 3 apically with a single spine and telopoditomere 4 with two spines or five spines on some specimens.

Posterior telopods (Figs 5A–D, 15E, F): With 4 telopoditomeres. First telopoditomere rectangular, longer than wide. Telopoditomere 2 large. Immovable finger (process of telopoditomere 2) long, massive, hammerlike, 2 times longer than wide, with a characteristic, apically extremely swollen, round, inner margin. With single spine; with thin dark spot near apex; tip *in situ*, curving ventrad; antero-apical margin a bit collapsed to accommodate tip of telopoditomere 4. Telopoditomere 3 stout; 2 times longer than wide, with single spine at excavate inner margin. Telopoditomere 4 relatively short, half as long as telopoditomere 3, strongly tapering toward apex; with two spines; immediately curved midway by forming a digitiform tip. Telopoditomeres 1 and 2 in anterior view covered by sparse setae, in posterior view glabrous. Telopoditomeres 3 and 4 glabrous. Inner horns with sharp tips, directed posteriad.

Female sexual characters (Fig. 4F): Vulva slightly short and slender; sparsely setose; covering almost 1/3 of coxa; extending mesally near base of prefemur. Operculum (op) round, slender, mesal margin protruding into a short, well-rounded lobe. Bursa (bu) relatively long, demarcated from operculum by a triangular groove.

Etymology. Named after Nong Hin District, where all specimens were collected. Adjective.

Distribution and habitat (Fig. 2G, H). *Sphaerobelum nonghinensis* sp. nov. is currently known only from the type locality in Nong Hin District, Loei Province. This new species was observed during the daytime in an evergreen forest within limestone habitat. Individuals typically conceal themselves beneath thick layers of leaf litter and decayed logs on rocky surfaces or in crevices, highlighting their adaptation to this unique environment.

Remarks. Females of *S. nonghinensis* sp. nov. are generally similar in size to males. This new species features a striking black body colour (but with contrasting orange markings on the thoracic shield and anal shield) and a telopod shape comparable to that of *S. onyx* sp. nov. However, genetic analysis reveals a notable difference, with a COI genetic divergence of 13.24% to 14.59%, indicating a significant level of separation between the two species.

Sphaerobelum onyx Srikampha & Srisonchai, sp. nov.

https://zoobank.org/EC4B72BB-607C-48EB-A2F9-0A44A7F4EA34

Figs 6–9, 14C, D, 15G, H, 16

Sphaerobelum sp. L10—Wesener, 2019: 239.

Type material. ***Holotype.*** Thailand • ♂ (MZKKU-MYR0003), Bueng Kan Province, Mueang District, Wat Phu Ngam (Wat Singhanat Banphot), 18°11'24.2"N, 103°50'40"E, ca. 180 m a.s.l., 11 August 2022, K. Srikampha, R. Srisonchai, and MZKKU students coll. ***Paratypes.*** THAILAND • 6 ♂♂, 5 ♀♀ (MZKKU-MYR0004), same data as holotype. • 4 ♂♂, 9 ♀♀ (MZKKU-MYR0004), 3 ♂♂, ♀ for SEM (MZKKU-MYR0004), Bueng Kan Province, Bueng Khong Long District, Wat Tham Puang, 17°58'10.9"N, 104°6'35.8"E, ca. 180 m a.s.l., 12 August 2022, K. Srikampha coll. • ♂ (CUMZ-MYR0032), same data as holotype. 1 ♂ (NHM), same data as holotype. • ♂ (NHMD), same data as holotype. • ♂ (NHMW), same data as holotype. • ♂, ♀ (ZFMK), same data as holotype.

Additional material examined—non-type. Thailand • 4 ♂♂ (MZKKU), Nakhon Phanom Province, Ban Phaeng District, Nakee Cave, Phu Langka National Park, 17°59'5.8"N, 104°7'38.3"E, ca. 320 m a.s.l., 12 August 2022, K. Srikampha coll. • ♂, 12 ♀♀ (MZKKU), Bueng

Figure 6. Photograph of live specimens of *Sphaerobelum onyx* sp. nov. **A–F.** Paratypes (MZKKU-MYR0004); **G, H.** Habitat at the type locality (sandstone). Scale bars: 10.0 mm.

Kan Province, Seka District, Wat Tham Chum Chang (Nam Yad Cliff), 18°11'29.6"N, 103°54'47"E, ca. 200 m a.s.l., 11 August 2022, K. Srikampha coll. • 7 ♂♂, 3 ♀♀ (MZKKU), Bueng Kan Province, Si Wilai District, Wat Pradu Nam Thip, 18°9'43"N, 103°51'34.9"E, ca. 200 m a.s.l., 11 August 2022, K. Srikampha coll. LAOS • ♀ (SMF), Vientiane Province, Vang Vieng, W. of Nam Song, Tham Nam or Khem, 18°55'46.86"N, 102°20'56.82"E, ca. 320 m a.s.l., 28 July 2014, P. Jäger & S. Münnich coll.

Diagnosis. *S. onyx* sp. nov. differs in the femur of the legs, in which only the apical margin carries a few teeth (no teeth or teeth at the entire margin in the other known *Sphaerobelum* species), a character only shared with *S. bicorne* Attems, 1938, *S. bolavensis* Wesener, 2019, *S. nonghinensis* sp. nov., as well as *S. petramurum* sp. nov. described below. *S. onyx* sp. nov. differs from both *S. bicorne* and *S. bolavensis* in the presence of a "hook" on telopoditomere 4 of the posterior telopods. *S. onyx*

sp. nov. differs by the glabrous tertgites (vs. hairy) from both *S. nonghinensis* sp. nov. and *S. petramurum* sp. nov. The black body colour with red appendages of *S. onyx* sp. nov. is unique for known Thai members of the genus but does also occur in *S. schwendingeri* Wesener, 2019, and *S. laoticum* Wesener, 2019, and potentially (known specimens are faded in ethanol) *S. peterjaegeri* Wesener, 2019, from Laos. *S. onyx* sp. nov. shares only with *S. clavigerum*, *S. hirsutum*, *S. laoticum*, *S. nonghinensis* sp. nov., *S. petramurum* sp. nov., *S. schwendingeri*, *S. separatum*, and *S. splendidum* the presence of a hook-like tip on telopoditomere 4 of the posterior telopods. *S. onyx* sp. nov. differs from *S. clavigerum* by having a shorter locking carina on anal shield (vs. 3× long), from *S. hirsutum* and *S. separatum* by glabrous tergites (vs. hairy), from *S. laoticum*, *S. nonghinensis* sp. nov., *S. petramurum* sp. nov., *S. schwendingeri*, and *S. splendidum* by the presence of 5–6 rows of marginal bristles and marginal bristles covering 3/4 of outer area (vs. 3–4 rows and 1/4 covered area).

Description. ***Measurements*:** Male holotype; body length 26.3 mm; width (broadest) of thoracic shield 13.5 mm of tergite 7 = 13.6 mm; height of tergite 7 = 7.2 mm. Males: body length = 23.7–26.1 mm; width (broadest) of thoracic shield = 11.9–13.3 mm, of tergite 7 = 12.2–13.7 mm; height of tergite 7 = 6.3–8.0 mm. Females: body length = 25.7–32.4 mm; width (broadest) of thoracic shield = 12.4–16.4 mm, of tergite 7 = 13.3–17.3 mm; height of tergite 7 = 8.2–10.0 mm.

Colouration (Fig. 6A–F): Live specimens with shiny black colour. Head, collum, thoracic shield, tergites, and anal shield black. Antennae, legs, and venter contrastingly brownish orange. Some specimens in alcohol after 3 years faded to dark brown; anterior margin of tergites and venter dark olive; legs brown.

Head (Fig. 7A, E): Trapeziform; with long and sparse setae, each seta located inside small pit. With 59–78 ommatidia (ocelli) in males and 71–85 in females. Aberrant ommatidium situated at brim of antennal groove. Organ of Tömösváry located at brim near the base of antenna, separated from eye field. No sclerotised crest/ridge between antennal socket and eye field.

Antennae (Figs 6B, C, 7A–D): Quite short; covered by long and dense setae; last antennomere extending back to leg pair 3 or 4. Lengths of antennomeres 6>1=2=3=4=5. Antennomere 6 slightly rounded apically, oval; apically with sensilla basiconica. Apical disc slightly convex, with 34–59 apical cones in male or 31–42 in female.

Epipharynx (Fig. 7F): With a regular central tooth (ct); laterally with abundant external teeth (et), short, triangular; inner area of each side with a row of dentate spines (rsp).

Gnathochilarium (Fig. 7G, H): Structure typical as for Sphaerotheriida. Lamellae linguales (ll) rectangular, apically truncate. Central pads (Cp) modified, with numerous sensory cones. Stipites (st) large; densely setose; located laterally to lamellae linguales. Mentum (me) large; fused at base; with dense and long setae. Lateral palpi inconspicuous. Inner palpi (ip) with sensory cones (sc) arranged in three fields (clusters).

***Mandibles* (gnathal lobe)** (Fig. 7I, J): With undivided external tooth (Et) and with conspicuous 3-combed inner tooth (3it). With 5–6 rows of pectinate lamellae (pl). Inner area (Ia) with group of tiny teeth. Molar plate (mp) flat, velvet-like; lacking a membranous fringe. Condylus (co) conspicuous, apically with one distinct ridge.

Tegument (Fig. 6A–F): Shiny and smooth; all tergites sparsely microscopic setose; each seta located in an inconspicuous pit. Anterior margins of midbody tergite and anal shield with a few rows of long setae.

Collum (Figs 6B, C, 7A): Subsemicircular; tip of lateral margin obtuse; sparsely long setose.

***Thoracic shield*:** With large and shallow groove demarcated by a large and long ridge at anterior edge. Groove and ridge smooth, without setae. Sloped towards groove with 3 inconspicuous (but traceable) keels.

***Midbody tergite*:** With a row of oval impressions at anterior margin. Tips of midbody paratergites projecting posteroventrad.

***Paratergites*:** Paratergites 3 and 4 slender, slightly attenuate; tip sharp. Paratergites 5–12 wide; tip obtuse.

***Anal shield*:** Slightly sexually dimorphic, in female large and well-rounded, in male slenderer. With a row of oval impressions at anterior edge. Underside without or with a single short or dot-like, black locking carina.

Endotergum of midbody tergite (Fig. 14C, D): Posterior margin (pm) unmodified, flat, regular. Outer area (oa) narrow; smooth, without setae. Marginal bristles arranged in five or six rows; tips of the longest bristles reaching to posterior margin (but not reaching above the margin). Middle area (ma) with several tiny cuticular impressions (cp), tubercle-like. Inner area (ia) without tubercles or setae.

***Pleurites* (laterotergites):** First pleurite slender, boomeranglike; apical margin slightly attenuated, strongly projecting into a wide tip. Pleurite 2 wider than the first one, tip obtuse. All remaining pleurites flat and broad, apical margin slightly extended.

Subanal plate (Fig. 8H): Densely setose; large and wide; subsemicircular; heartlike; apical; apical margin strongly concave.

Stigmatic plates (Fig. 8C, D): First stigmatic plate slender, apex rounded. Second stigmatic plate in both sexes not curved.

Legs (Fig. 8A–G): All podomeres sparsely setose. Coxa (cx) large; coxal process absent in first legs; each side of legs 2–21 laterally with a dentate ridge. Prefemur (pre) quite short; apico-mesally with short but conspicuous projection. Femur (fe) 1.8 times longer than wide, with a long ridge in all leg pairs; apico-mesally with inconspicuous dentate margin, carrying inconspicuous teeth (Sp). Postfemur (po) and tibia (ti) relatively short. Tarsus (ta) of midbody legs quite long, 3.9 times longer than wide, as long as length of femur+postfemur; first two leg pairs without apical spine; leg-pair 1 with 2 ventral spines; leg-pair 2 with 4 ventral spines; leg-pair 3 with 6 or 7 ventral spines and 1 apical spine; leg pairs 4–21 with 6 or 8 ventral spines and 1 apical spine. Claw normal, with a small notch at base.

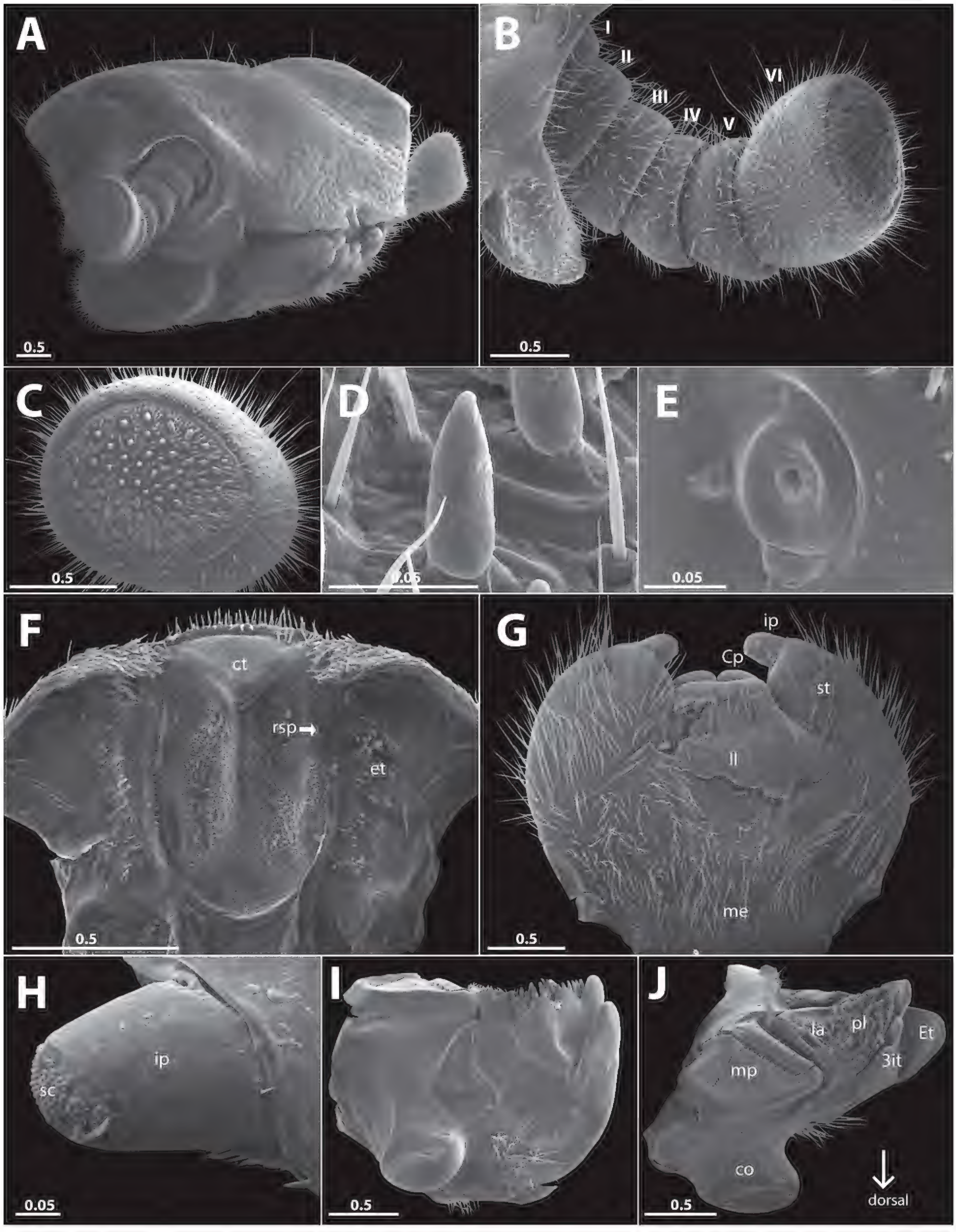

Figure 7. SEM of *Sphaerobelum onyx* sp. nov., ♂ paratype (MZKKU-MYR0004). **A.** Head region, lateral view; **B.** Left antenna, anterior view; **C.** Antennal disc, anterior view; **D.** Apical cones on antennal disc, lateral view; **E.** Organ of Tömösváry, lateral view; **F.** Epipharynx, ventral view; **G.** Gnathochilarium, ventral view; **H.** Sensory cones on inner palpi, anterior view; **I, J.** Mandible, anterior and mesal views, respectively. Abbreviations: 3it = 3-combed inner tooth, co = condylus, cp = central pad, ct = central tooth, et = external tooth, Et = external tooth, Ia = inner area, ip = inner palpi, ll = lamellae linguales, me = mentum, mp = molar plate, pl = pectinate lamellae, rsp = row of spines, sc = sensory cone, st = stipite. Scale bars in millimetres.

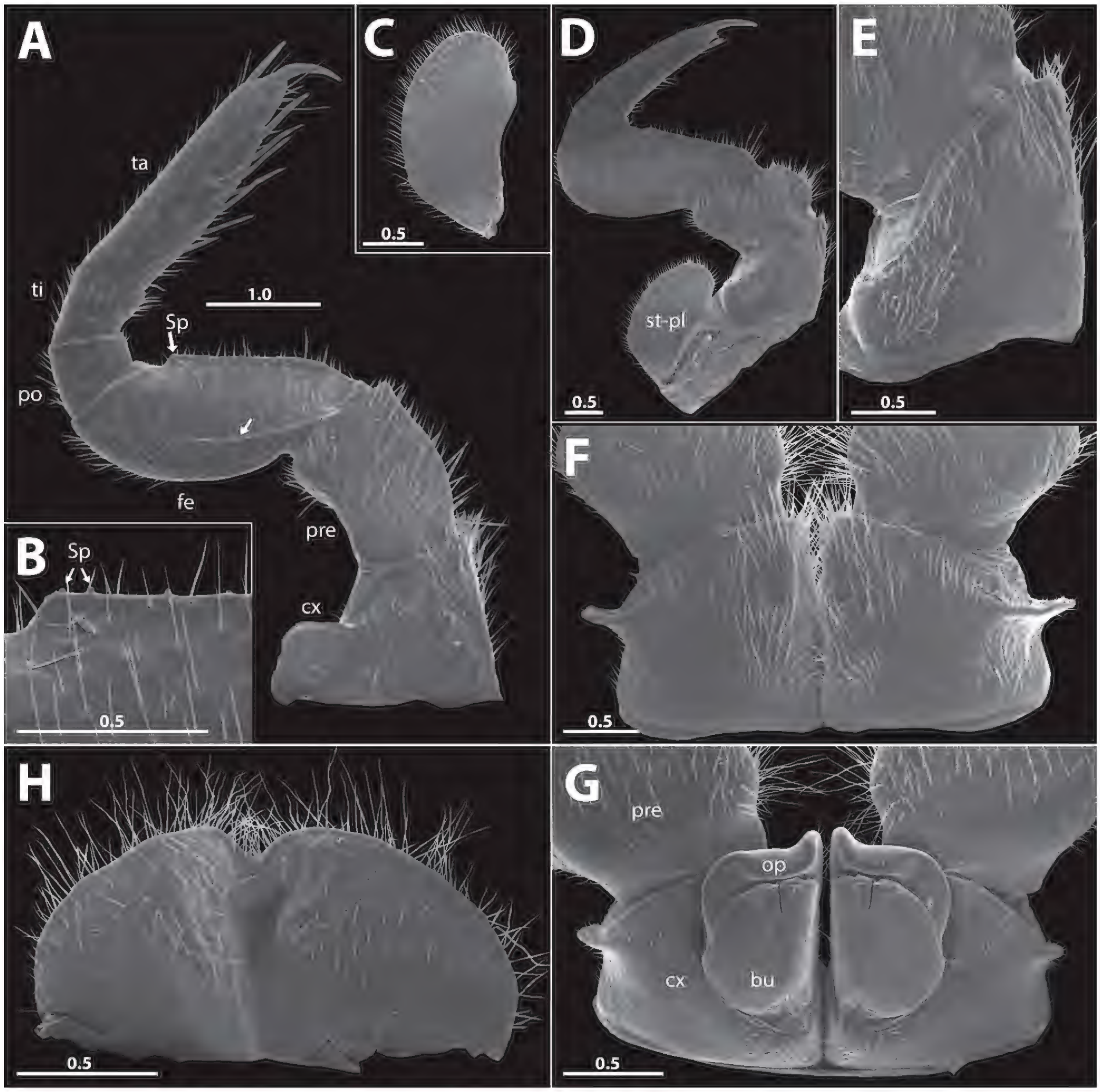

Figure 8. SEM of *Sphaerobelum onyx* sp. nov. **A–F.** ♂ paratype (MZKKU-MYR0004); **G, H.** ♀ paratype (MZKKU-MYR0004). **A.** Leg 11, arrow points to femoral ridge; **B.** Small spines on femur; **C.** Stigmatic plate 1; **D.** Legs 1 with stigmatic plate; **E.** Coxa of legs 1; **F.** Coxae of legs 2 with gonopores; **G.** Leg 2 with vulvae; **H.** Subanal plate. Abbreviation: bu = bursa, cx = coxa, fe = femur, op = operculum, po = postfemur, pre = prefemur, Sp = apico-mesally spine of leg, st-pl = stigmatic plate, ta = tarsus, ti = tibia. Scale bars in millimetres.

Male gonopore (Fig. 8F): Small, triangular; covered by long setae.

Anterior telopods (Fig. 9A, C, E–G): First telopoditomere rectangular. Telopoditomere 2 large and stout, with process as long as telopoditomere 1. Immovable finger (process of telopoditomere 2) slightly long; almost as long as telopoditomere 3; strongly curved; tip obtuse, inner margin with single spine. Telopoditomere 3 longer than telopoditomere 4, clearly demarcated from telopoditomere 4 by suture when seen in ventral view, apically with one spine. Tepoloditomere 4 short, less than half as long as telopoditomere 3, with two small spines; tip directed mesad.

Posterior telopods (Figs 9A–D, 15G, H): Consisting of 4 telopoditomeres. First telopoditomere rectangular, length = width. Telopoditomere 2 large and stout. Immovable finger (process of telopoditomere 2) quite long, hammerlike; 2 times longer than wide, with a characteristic, extremely swollen, apically round apex; tip obtuse; with thick and dark spot near apex; tip *in situ*, curving ventrad; antero-apical margin a bit collapsed to accommodate tip of telopoditomere 4. Telopoditomere 3 quite short, 2 times longer than wide, with a single spine at excavated inner margin. Telopoditomere 4 short, 3 times shorter than telopoditomere 3, with two spines, strongly tapering toward apex and slightly curved near apex by forming a digitiform tip. Telopoditomeres 1 and 2 in anterior and posterior views mostly covered by setae. Telopoditomeres 3

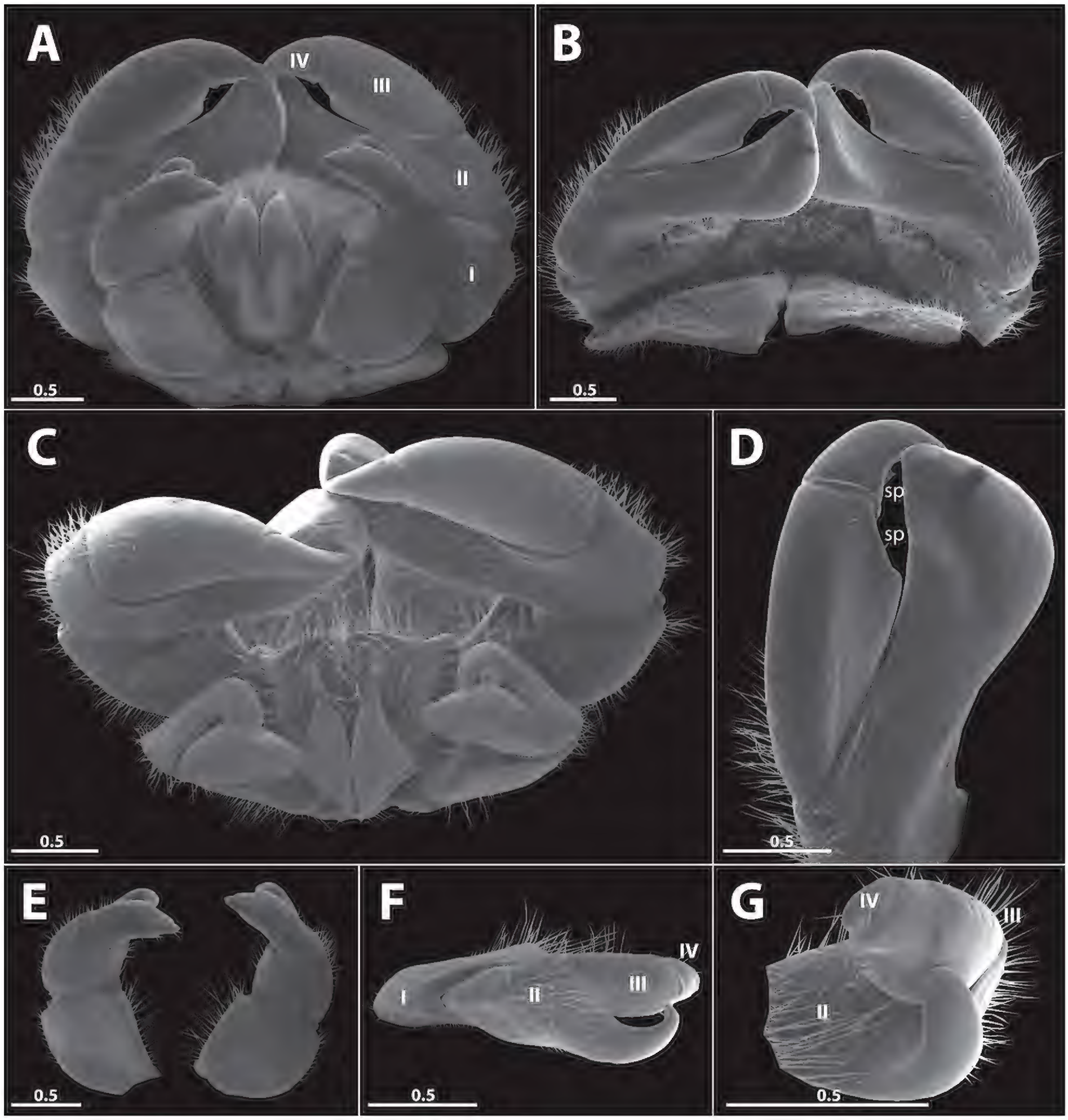

Figure 9. SEM of *Sphaerobelum onyx* sp. nov., ♂ paratype (MZKKU-MYR0004). **A–C.** Telopods, anterior, posterior, and ventral views, respectively; **D.** Right posterior telopod, posterior view; **E–G.** Anterior telopod, anterior, sublateral, and subventral views, respectively. Abbreviations: sp = telopoditomere 4 of posterior telopod's spine. Scale bars in millimetres.

and 4 mostly glabrous, except small area at basal part of telopoditomere 3 with long setae. Inner horns with sharp-edged tips.

Female sexual characters (Fig. 8G): Vulva short and stout; sparsely setose; covering almost 1/3 of coxa; projecting mesally to base of prefemur. Operculum (op) narrow, flattened dorso-ventrally when seen in posterior view; mesal margin protruding into a small lobe on each side. Bursa (bu) short and stout, demarcated from operculum by a triangular groove.

Etymology. The name is a noun in apposition and refers to the remarkable black body colour, which somewhat resembles the chalcedony mineral "onyx."

Distribution and habitat (Fig. 6G, H). *Sphaerobelum onyx* sp. nov. is currently known from the Mekong River basin, specifically in Laos and Thailand. All examined specimens in Thailand (Bueng Khan and Nakhon Phanom Districts) were observed during the daytime on rocky sandstone beds that were covered with thick leaf litter in evergreen forests. Notably, a single female previously reported by Wesener (2019) was found in limestone habitats in the Vang Vieng district (18°55'46.9"N, 102°20'56.8"E), indicating some habitat variability within its distribution.

Remarks. Wesener (2019) identified a single female specimen from Vang Vieng, Laos, as *Sphaerobelum* sp. L10, although it has not yet been formally named. The

morphology of all the newly collected specimens from Thailand corresponds closely with the description of this female specimen, showing a genetic divergence of 5.02% based on the COI genetic divergence.

In this species, females typically exhibit a larger body size compared to males. Additionally, some specimens display variation in the locking carina, which may be absent or consist of a single short or dot-like structure.

Sphaerobelum petramurum Srikampha & Srisonchai, sp. nov.

https://zoobank.org/A65CB124-F17B-4BD2-9E9C-957C0A4E2442

Figs 10–12, 14E, F, 15I, J, 16

Type material. ***Holotype.*** Thailand • ♂ (MZKKU-MYR0005) Khon Kaen Province, Phu Pha Man District, Ban Khao Wong, 16°38'30.5"N, 101°46'37"E, ca. 247 m. a.s.l., 23 June 2022, K. Srikampha, R. Srisonchai, and MZKKU students coll. ***Paratypes.*** Thailand• ♂, ♀ for SEM (MZKKU-MYR0006), same data as holotype. • ♂, 2 ♀♀ (MZKKU-MYR0006), same data as holotype, 16 May 2021. • 3 ♂♂ (MZKKU-MYR0006), same data as holotype, 26 September 2021. • ♂, 2 ♀♀ (MZKKU-MYR0006), same data as holotype, 23 September 2023. • 3 ♂♂, 8 ♀♀ (MZKKU-MYR0006), same data as holotype, 8 October 2023.

Additional material examined—non-type. Thailand • 3 ♂♂, 2 ♀♀ (MZKKU), Khon Kaen Province, Phu Pha Man District, Ban Sam Poep, 16°40'44.2"N, 101°52'10"E, ca. 277 m. a.s.l., 17 May 2021. K. Srikampha coll. • ♀ (MZKKU), Khon Kaen Province, Phu Pha Man District, Ban Sam Poep, 16°40'44.2"N, 101°52'10"E, ca. 277 m. a.s.l., 23 June 2022. K. Srikampha coll. • 2 ♂♂ (MZKKU), ♂ (CUMZ-MYR0033), ♂ (NHM), ♂ (NHMD), ♂ (NHMW), ♂ (ZFMK), Khon Kaen Province, Phu Pha Man District, Wat Si Walee Sattha Tham, 16°39'18.0"N, 101°52'14.5"E, ca. 260 m. a.s.l., 1 June 2024. K. Srikampha coll. • ♀ (MZKKU), Khon Kaen Province, Phu Pha Man District, Wat Si Walee Sattha Tham, 16°39'18.0"N, 101°52'14.5"E, ca. 260 m. a.s.l., 14 September 2024. K. Srikampha coll. • 3 ♂♂, ♀ (MZKKU), Khon Kaen Province, Si Chomphu District, Wat Tham Saeng Tham, 16°50'31.0"N, 102°03'56.2"E, ca. 270 m. a.s.l., 27 May 2024. K. Srikampha coll. • 6 ♂♂, 4 ♀♀ (MZKKU), Khon Kaen Province, Si Chomphu District, Wat Tham Sing to Thong, 16°47'55.9"N, 102°02'49.3"E, ca. 360 m. a.s.l., 27 May 2024. K. Srikampha coll. • ♀ (MZKKU), Chaiyaphum Province, Khon San District, Mortagek Monastery, 16°30'17.0"N, 101°50'41.8"E, ca. 390 m. a.s.l., 16 July 2023. K. Srikampha coll. • ♂ (MZKKU), Chaiyaphum Province, Khon San District, Wat Tham Phaya Chang Phueak, 16°33'47.6"N, 101°51'36.3"E, ca. 320 m. a.s.l., 1 June 2024. K. Srikampha coll.

Diagnosis. *S. petramurum* sp. nov. differs in the femur of the legs, in which only the apical margin carries a few teeth (no teeth or teeth at the entire margin in the other known *Sphaerobelum* species), a character only shared with *S. bicorne* Attems, 1938, *S. bolavensis* Wesener, 2019, *S. nonghinensis* sp. nov., and *S. onyx* sp. nov. *S. petramurum* sp. nov. differs from both *S. bicorne* and *S. bolavensis* in the presence of a "hook" on telopoditomere 4 of the posterior telopods. *S. petramurum* sp. nov. differs strongly in the colouration from both *S. nonghinensis* sp. nov. and *S. onyx* sp. nov. (greenish-bluish brown vs. black).

S. petramurum sp. nov. shares only with *S. clavigerum*, *S. hirsutum*, *S. laoticum*, *S. nonghinensis* sp. nov., *S. onyx* sp. nov., *S. schwendingeri*, *S. separatum*, and *S. splendidum* the presence of a "hook" on telopoditomere 4 of the posterior telopods. This new species differs from *S. clavigerum* by having a single short or dot-like locking carina on the anal shield (vs. 3× long), from *S. hirsutum* and *S. separatum* in the presence of glabrous tergites (vs. hairy). It also differs from *S. laoticum* and *S. schwendingeri* in the presence of apical dish carrying < 60 apical cones and tergites greenish-bluish brown (vs. 81–86 in *S. laoticum*, 36–73 in *S. schwendingeri*, and tergites black), from *S. splendidum* in the presence of leg 2 with coxal process (vs. absent) and a long telopoditomere 2 of anterior telopod (vs. short, without process as long as telopoditomere 3), and from *S. nonghinensis* sp. nov. by having a greenish-bluish brown body colour (vs. almost black). It differs from *S. onyx* sp. nov. by the presence of 5–6 rows of marginal bristles and marginal bristles covering 3/4 of outer area (vs. 3–4 rows, 1/4 cover area).

Description. ***Measurements*:** Male holotype; body length 29.1 mm, width (broadest) of thoracic shield 13.7 mm, of tergite 7 = 14.5 mm; height of tergite 7 = 8.5 mm. Males: body length = 25.7–25.9 mm; width (broadest) of thoracic shield = 13.0–13.7 mm, of tergite 7 = 13.9–14.7 mm; height of tergite 7 = 8.3–8.9 mm. Females: body length = 29.7–30.5 mm; width (broadest) of thoracic shield = 14.5–15.3 mm, of tergite 7 = 15.3–16.2 mm; height of tergite 7 = 9.2–10.0 mm.

Colouration (Fig. 10A–G): Specimens in life greenish-bluish brown or light brown, shiny. Head and collum brown to dark brown. Antennae, thoracic shield, paratergites, anal shield, legs, and venter light brown. Midbody area of each tergite with a longitudinal bluish-green or brown stripe (band), becoming visible when the animal rolls up. Lateral margin of each tergite with a brown patch. Anal shield with a large triangular brown patch. Specimens in alcohol after 3 years slightly faded to pale greenish-bluish brown.

Head (Fig. 11A, E): Trapeziform; densely setose in anterior part and sparsely setose in posterior one; each seta located inside small pit. With 66–83 ommatidia (ocelli) in males and 54–79 in females. Aberrant ommatidium and organ of Tömösváry as in *S. nonghinensis* sp. nov. and *S. onyx* sp. nov.

Antennae (Figs 10B, C, 11B–D): Quite short and slender; covered by long and dense setae; last antennomere reaching back to leg pair 2 or 3. Lengths of antennomeres 6>1=2=3=4=5 Antennomere 6 rounded apically; oval; apically with sensilla basiconica. Apical disc slightly convex, with 49–56 apical cones in male or 27–32 in female.

Epipharynx (Fig. 11F): With a regular central tooth (ct); laterally with numerous external teeth (et), short and sharp; inner area of each side with a row of delicately dentate spines (rsp).

Gnathochilarium (Fig. 11G, H): Structure typical as for Sphaerotheriida. Lamellae linguales (ll) rectangular,

Figure 10. Photograph of live specimens of *Sphaerobelum petramurum* sp. nov. **A–G.** Paratypes (MZKKU-MYR0006); **H.** Habitat at the type locality (limestone). Scale bars = 10.0 mm.

apically truncate. Central pads (Cp) modified, with numerous sensory cones. Stipites (st) large; densely setose; located laterally to lamellae linguales. Mentum (me) large; fused at base; with dense and long setae. Lateral palpi inconspicuous. Inner palpi (ip) with sensory cones (sc) arranged in three fields (clusters).

Mandibles **(gnathal lobe)** (Fig. 11I): With undivided external tooth (Et) and with conspicuous 3-combed inner tooth (3it). With 5–6 rows of pectinate lamellae (pl). Inner area (Ia) with group of tiny teeth. Molar plate (mp) flat, velvet-like; lacking a membranous fringe. Condylus (co) apically with two or three ridges.

Tegument (Fig. 10A–G): Shiny; all tergites sparsely microscopic setose; each seta located in an inconspicuous pit. Anterior margins of midbody tergite and anal shield with a few rows of long setae.

Collum (Figs 10B, C, 11A): Subsemicircular; tip of lateral margin obtuse; sparsely long setose at margin.

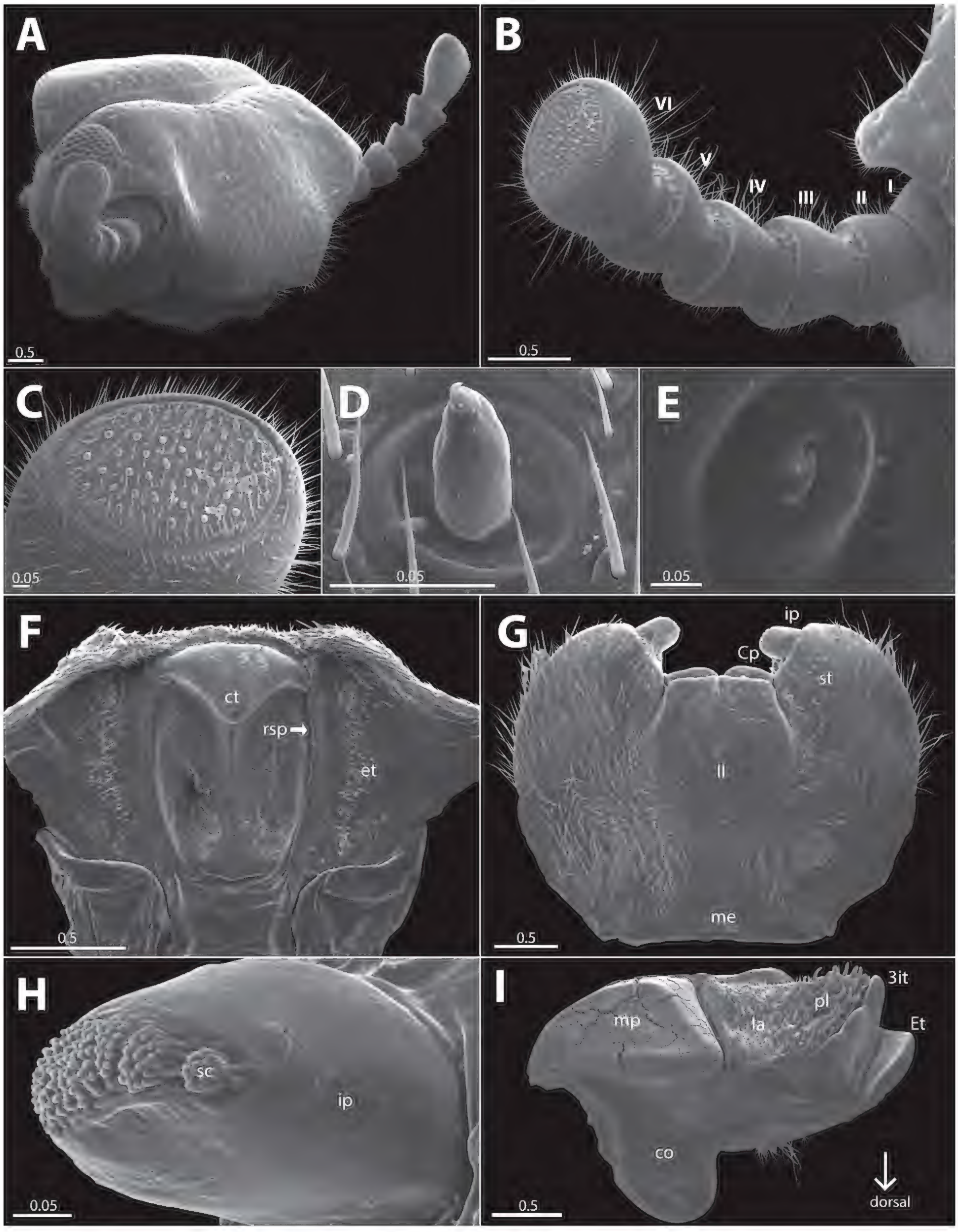

Figure 11. SEM of *Sphaerobelum petramurum* sp. nov. **A–E.** ♂ paratype (MZKKU-MYR0006); **F–I.** ♀ paratype (MZKKU-MYR0006). **A.** Head region, lateral view; **B.** Right antenna, anterior view; **C.** Antennal disc, anterior view; **D.** Apical cones on antennal disc, lateral view; **E.** Organ of Tömösváry, lateral view; **F.** Epipharynx, ventral view; **G.** Gnathochilarium, ventral view; **H.** Sensory cones on inner palpi, anterior view; **I.** Mandible, mesal view. Abbreviations: 3it = 3-combed inner tooth, co = condylus, Cp = central pad, ct = central tooth, et = external tooth, Et = external tooth, Ia = inner area, ip = inner palpi, ll = lamellae linguales, me = mentum, mp = molar plate, pl = pectinate lamellae, rsp = row of spines, sc = sensory cone, st = stipite. Scale bars in millimetres.

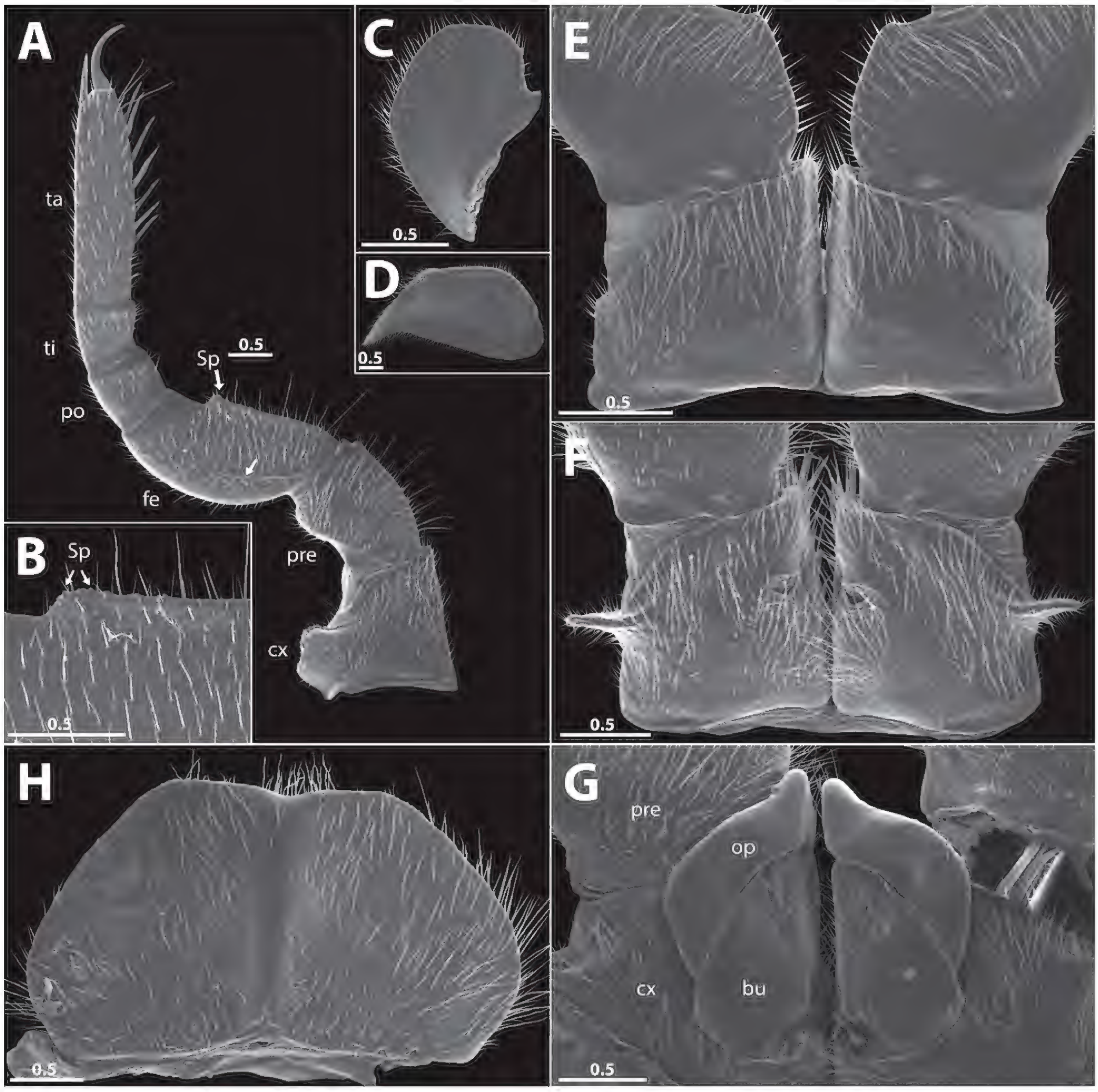

Figure 12. SEM of *Sphaerobelum petramurum* sp. nov. **A–F.** ♂ paratype (MZKKU-MYR0006); **G, H.** ♀ paratype (MZKKU-MYR0006). **A.** Leg 11, arrow points to femoral ridge; **B.** Small spine on femur; **C.** Stigmatic plate 1; **D.** First pleurite; **E.** Coxae of legs 1; **F.** Coxae of legs 2 with gonopores; **G.** Leg 2 with vulvae; **H.** Subanal plate. Abbreviation: bu = bursa, cx = coxa, fe = femur, op = operculum, po = postfemur, pre = prefemur, Sp = apico-mesally spine of leg, ta = tarsus, ti = tibia. Scale bars in millimetres.

***Thoracic shield*:** Anteriorly with shallow and large grooves separated by a long ridge. Groove and ridge smooth, without setae. Sloped towards groove laterally with 4 inconspicuous keels.

***Midbody tergite*:** With a row of oval impressions at anterior margin. Tips of midbody paratergites projecting posteroventrad.

***Paratergites*:** Paratergites 3 and 4 slender, slightly attenuate; tip sharp. Paratergites 5–12 wide; tip obtuse.

***Anal shield*:** Slightly sexually dimorphic; large and well-rounded in female, slenderer in male. Underside with a single, black locking carina; twice as long as length of tergites.

Endotergum of midbody tergite (Fig. 14E, F): Posterior margin (pm) unmodified, flat, regular. Outer area (oa) quite wide; smooth, without setae. Marginal bristles arranged in three or four rows; tips of the longest bristles not protruding above posterior margin. Middle area (ma) with a single row of conspicuous, wavy impressions; distance between impressions twice as long as individual diameter. Inner area (ia) without tubercles or setae.

***Pleurites* (laterotergites)** (Fig. 12D): First pleurite slender, boomeranglike; apical margin attenuated, strongly projecting into a wide tip. Pleurite 2 wider than the first one, protruding into obtuse tip. All remaining pleurites flat and broad, apical margin slightly extended.

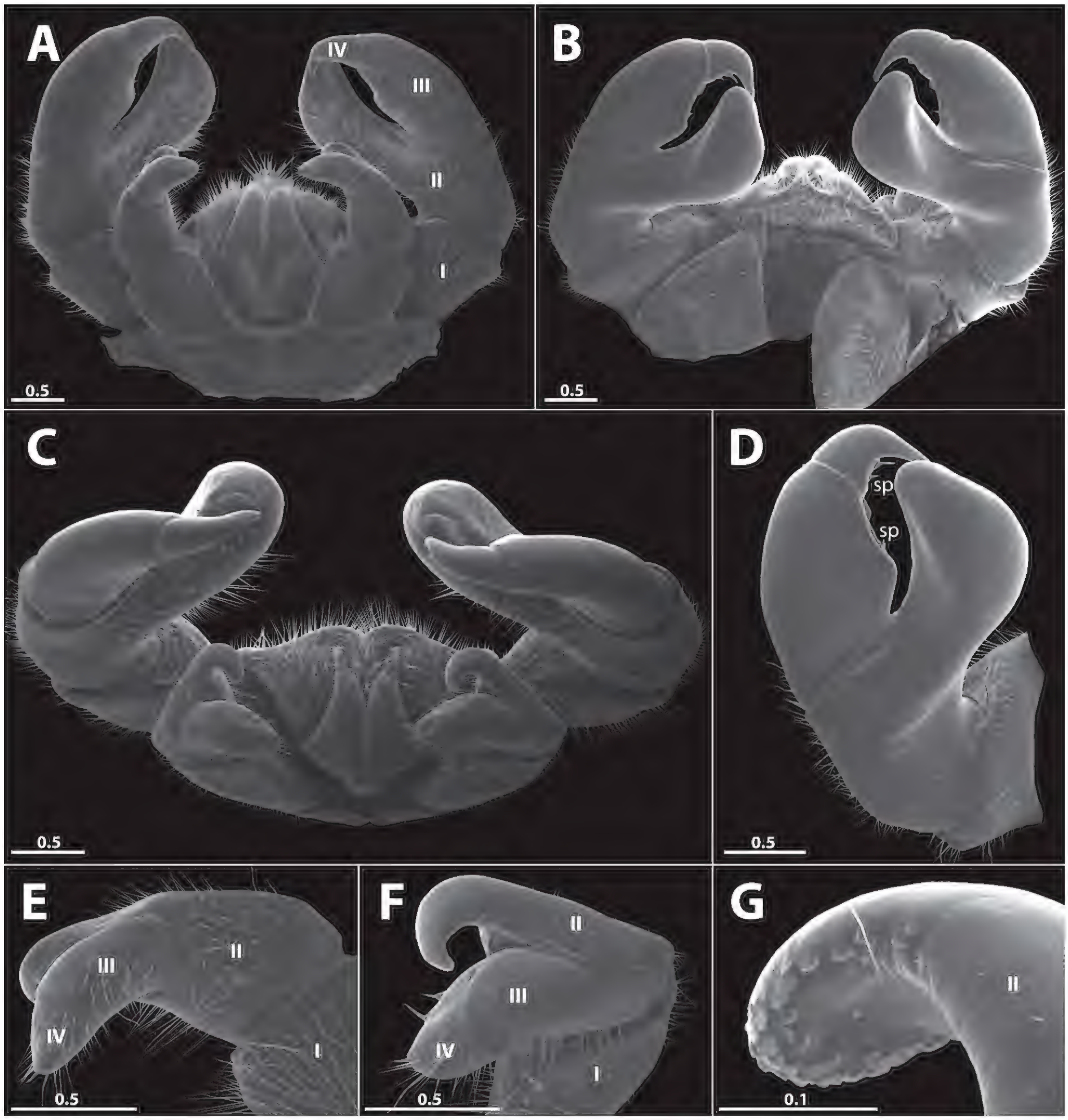

Figure 13. SEM of *Sphaerobelum petramurum* sp. nov., ♂ paratype (MZKKU-MYR0006). **A–C.** Telopods, anterior view, posterior view, and ventral views, respectively; **D.** Right posterior telopod, posterior view; **E–G.** Right anterior telopod, anterior, sublateral, and subdorsal views, respectively. Abbreviations: sp = telopoditomere 4 of posterior telopod's spine. Scale bars in millimetres.

Subanal plate (Fig. 12H): Densely setose; broad and wide; subsemicircular; apical margin slightly concave.

Stigmatic plates (Fig. 12C): First stigmatic plate trapeziform, apex rounded. Second stigmatic plate in both sexes not curved.

Legs (Fig. 12A–G): All podomeres sparsely setose. Coxa (cx) large; coxal process absent in first legs; each side of legs 4–21 marginally with a large, dentate ridge. Prefemur (pre) quite short; apico-mesally with a weak projection. Femur (fe) 1.8 times longer than wide, with long ridge in all leg pairs; apico-mesally with inconspicuous dentate margin, carrying inconspicuous teeth (Sp). Postfemur (po) and tibia (ti) short. Tarsus (ta) of midbody legs quite long, 4 times longer than wide, as long as length of femur+postfemur; first two leg pairs without an apical spine; leg-pair 1 with 2 ventral spines; leg-pair 2 with 4 or 5 ventral spines; leg-pair 3 with 6 or 7 ventral spines and 1 apical spine; leg pairs 4–21 with 6 or 7 ventral spines and 1 apical spine. Claw normal, with a small notch at base.

Male gonopore (Fig. 12F): Small, triangular; covered by long setae.

Anterior telopods (Fig. 13A, C, E–G): First telopoditomere rectangular, slender, width < height. Telopoditomere 2 large, longer than telopoditomere 1. Immovable finger (process of telopoditomere 2) long and slender, longer than telopoditomere 3, clearly seen in posterior and

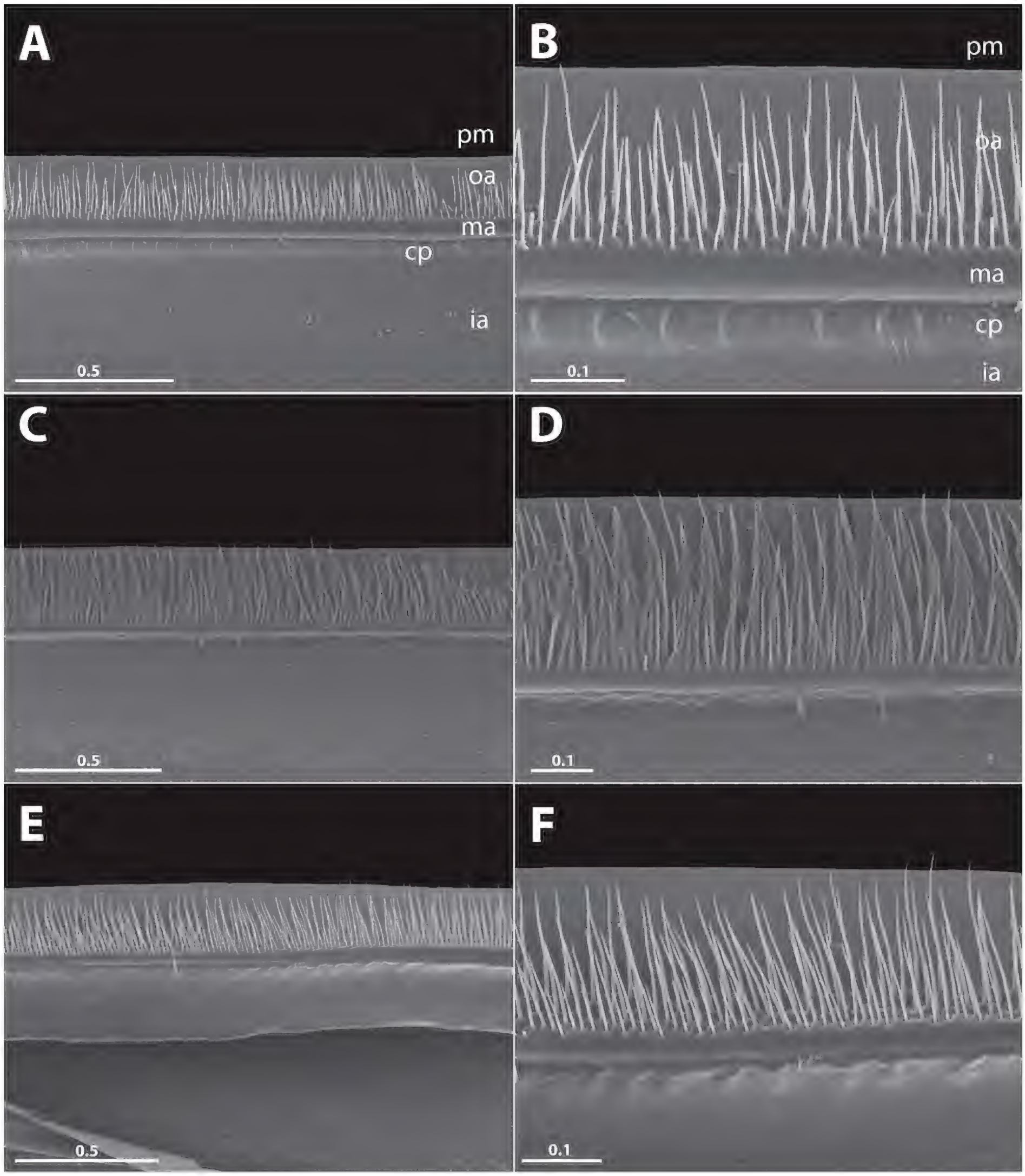

Figure 14. SEM of endoterga of midbody tergites. **A, B.** *Sphaerobelum nonghinensis* sp. nov. (♂ paratype, MZKKU-MYR0002); **C, D.** *Sphaerobelum onyx* sp. nov. (♂ paratype, MZKKU-MYR0004); **E, F.** *Sphaerobelum petramurum* sp. nov. (♂paratype, MZKKU-MYR0006). Abbreviations: cp = cuticular impression, ia = inner area, ma = middle area, oa = outer area, pm = posterior margin. Scale bars in millimetres.

ventral views, strongly curved; tip obtuse, apically with several sclerotised spots. Telopoditomere 3 longer than telopoditomere 4, distinctly demarcated from telopoditomere 4 by suture when seen in ventral view, apically with a single spine. Tepoloditomere 4 short, less than half as long as telopoditomere 3, with three spines (two spines located near base and one at apex); tip directed mesad.

Posterior telopods (Figs 13A–D, 15I, J): Slender. Consisting of 4 telopoditomeres. First telopoditomere rectangular. Telopoditomere 2 large and long. Immovable finger (process of telopoditomere 2) long, hammer-like; 2 times longer than wide, with a characteristic, mesally swollen apex; tip obtuse, with thick and dark spot near apex; *in-situ* curving ventrad; antero-apical margin slightly collapsed to accommodate tip of telopoditomere 4; inner margin with single spine. Telopoditomere 3 quite short, 2 times longer than wide, with single spine at excavated inner margin. Telopoditomere 4 relatively short, 2 times

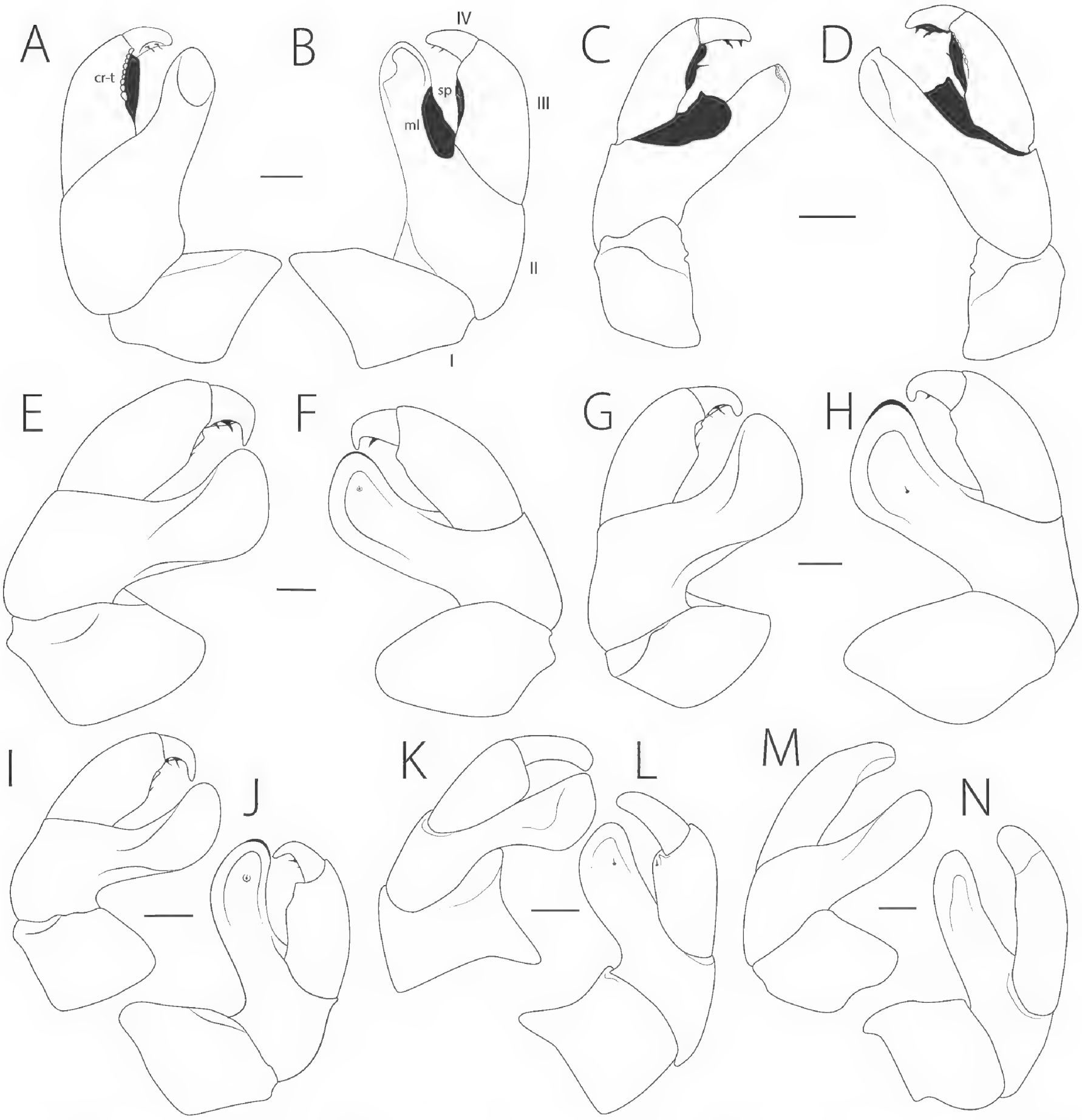

Figure 15. Line drawings of posterior telopods of *Sphaerobelum* species in Thailand. **A, B.** *Sphaerobelum aesculus*; **C, D.** *Sphaerobelum meridionalis*, modified from Bhansali & Wesener, 2022; **E, F.** *Sphaerobelum nonghinensis* sp. nov.; **G, H.** *Sphaerobelum onyx* sp. nov.; **I, J.** *Sphaerobelum petramurum* sp. nov.; **K, L.** *Sphaerobelum truncatum*; **M, N.** *Sphaerobelum turcosa*. **A, B, E–N.** Right posterior telopods; **C, D.** Left posterior telopods. **A, D, E, G, I, K, M.** Posterior view; **B, C, F, H, J, L, N.** Anterior view. Abbreviations: cr-t = crenulated teeth, ml = membranous lobe, sp = spine on telopoditomere 4 of posterior telopod. Scale bar: 0.5 millimetres.

shorter than telopoditomere 3, strongly tapering toward apex; slightly curved toward apex by forming a digitiform tip with two long spines. Telopoditomere 1 covered by setae. Telopoditomeres 2 with setae only in anterior view. Telopoditomeres 3 and 4 glabrous, except small area at basal part of telopoditomere 3. Inner horns with sharp-edged tips, slightly curved caudad.

Female sexual characters (Fig. 12G): Vulva quite long and slender. Vulva large, slender; covering almost 1/3 of coxa; extending mesally to almost half of prefemur. Operculum (op) wide and slender; mesal margin strongly protruding into an obtuse lobe on each side. Bursa (bu) long and slender, demarcated from operculum by a triangular groove.

Etymology. The name is a Latin noun, here in apposition, meaning "rock wall," and refers to the preferred habitat of the new species found in limestone.

Distribution and habitat (Fig. 10H). *Sphaerobelum petramurum* sp. nov. is currently distributed in limestone borders of Chaiyaphum and Khon Kaen Provinces. Most specimens have been discovered exclusively in small crevices within rocky walls or beds in humid limestone evergreen forests. This unique habitat highlights the adaptation to its specific environment, where moisture and shelter are abundant, allowing it to thrive in these limestone-rich ecosystems.

Remarks. The intraspecific genetic divergence (*p*-distance) of the COI fragment in the new species is high,

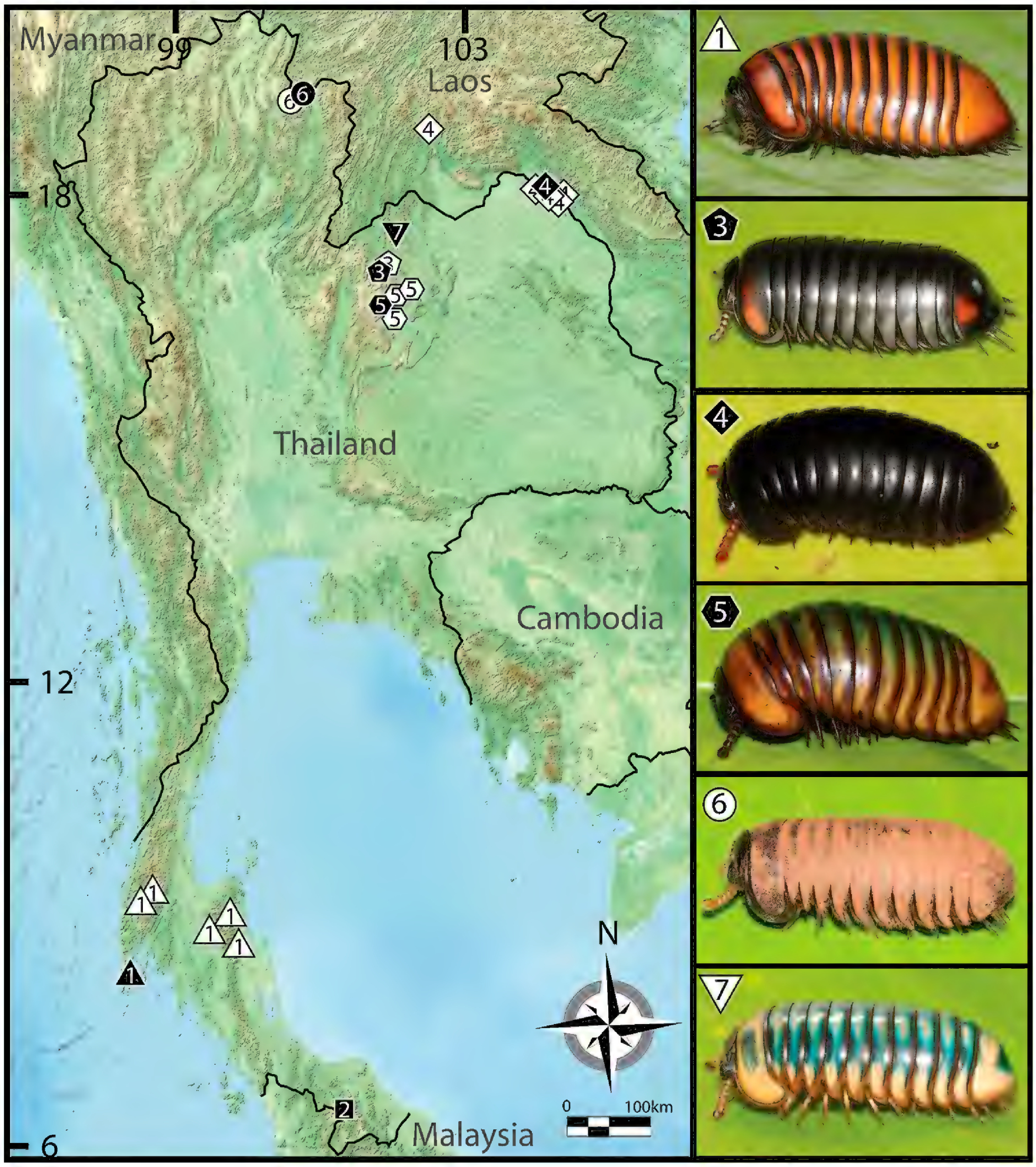

Figure 16. Distribution map of *Sphaerobelum* species in Thailand. Different symbols with numbers represent species: 1 = *S. aesculus*, 2 = *S. meridionalis*, 3 = *S. nonghinensis* sp. nov., 4 = *S. onyx* sp. nov., 5 = *S. petramurum* sp. nov., 6 = *S. truncatum*, 7 = *S. turcosa*. Black symbol = type locality; white symbol = other locality.

ranging from 0 to 7.15%, as observed between the populations of the Mortagek Monastery and others.

The majority of specimens display a greenish-brown body colour, while a minority exhibit a light brown colour, with both variants found within the same populations. Females are typically larger in size than males.

Sphaerobelum truncatum Wongthamwanich, 2012

Figs 15K, L, 16

Sphaerobelum truncatum Wongthamwanich, 2012 in Wongthamwanich et al. 2012: 34.

Sphaerobelum truncatum—Wesener 2016: 36; Semenyuk et al. 2018: 543; Wesener 2019: 211; Likhitrakarn et al. 2023: 55; Srisonchai et al. 2023: 52.

New material examined. Thailand • ♂ (MZKKU), Phayao Province, Pong District, Tham Phra-Sakern Monastery, 620 m a.s.l., 19°21'56.2"N, 100°31'51.3"E, 2 October 2023, K. Srikampha & T. Benchapong coll.

Distribution. This species occurs only in a small area near the Nan-Phayao border. The new specimen was collected from limestone habitats, whereas the type materials were found in montane evergreen-bamboo forest.

Sphaerobelum turcosa Srisonchai & Pimvichai, 2023

Figs 15M, N, 16

Sphaerobelum turcosa Srisonchai & Pimvichai, 2023 in Srisonchai et al. 2023: 45.

New material examined. Thailand • 2 ♂♂ (MZKKU), Loei Province, Mueang Loei District, Phu Pha Lom Forest Park, 540 m a.s.l., 17°34'18.4"N, 101°52'18.0"E, 18 September 2023, P. Sukkharom coll.

Distribution. This species is known only from the type locality, which is characterised by the highly irregular geomorphology of limestone habitat at Phu Pha Lom Forest Park in Loei Province. Based on our observations of specimens at both the forest floor and on rocks, we suggest that this species is likely inhabiting only rock crevices or walls.

Key to species of the genus *Sphaerobelum* in Thailand (7 species)

1 Tarsus of legs 4–21 usually with one apical spine (Figs 4A, 8A, 12A). Posterior telopods: immovable finger of telopoditomere 2 without membranous spot (Fig. 15E–N) 2
– Tarsus of legs 4–21 usually with three apical spines. Posterior telopods: immovable finger of telopoditomere 2 with membranous spot, visible in posterior view (Fig. 15A, D) 6
2 Posterior telopods: telopoditomere 4 hook-like (Fig. 15E–J)..... 3
– Posterior telopods: telopoditomere 4 cylindrical in shape (Fig. 15K–N)..... 5
3 Body mostly shiny black (Figs 2A–F, 6A–F). Vulva quite stout (Figs 4F, 8G) 4
– Body greenish bluish brown, shiny (Fig. 10). Vulva slenderer (Fig. 12G)..... *S. petramurum* sp. nov.
4 Antenna, podomere and venter olive green (Fig. 2B, C). Black thoracic shield and anal shield with contrasting orange markings. Endotergum with 3 or 4 rows of bristles (Fig. 14A, B). Telopoditomere 3 indistinctly demarcated from telopoditomere 4 (Fig. 5F). Operculum of vulva wide, tip short (Fig. 4F) ..... *S. nonghinensis* sp. nov.
– Antenna, podomere and venter bright orange (Fig. 6B, C). Thoracic shield and anal shield entirely black. Endotergum with 5 or 6 rows of bristles (Fig. 14C, D). Telopoditomere 3 distinctly demarcated from telopoditomere 4 (Fig. 9F). Operculum of vulva narrow, tip slightly elongate (Fig. 8G) ..... *S. onyx* sp. nov.
5 Endotergum with regular, flat posterior margin. Leg 3 without an apical spine. Coxa of second leg laterally with a sharp and long process. Telopoditomere 4 of anterior telopod with three separated spines. Posterior telopods: immovable finger of telopoditomere 2 more swollen; telopoditomere 4 shorter (Fig. 15M, N)..... *S. turcosa* Srisonchai & Pimvichai, 2023
– Endotergum with rectangular-wavy posterior margin. Leg 3 with one apical spine. Coxa of second leg laterally without process. Telopoditomere 4 of anterior telopod with two separated spines. Posterior telopods: immovable finger of telopoditomere 2 more slender; telopoditomere 4 longer (Fig. 15K, L) ..... *S. truncatum* Wongthamwanich, 2012
6 Endotergum with two rows of bristles. First coxae with mesal process. Prefemur of midbody legs with mesal process. Telopoditomeres 3 and 4 of anterior telopods clearly demarcated from each other in all views..... *S. meridionalis* Bhansali & Wesener, 2022
– Endotergum with one row of bristles. First coxa without mesal process. Prefemur of midbody legs without mesal process. Telopoditomere 3 and 4 of anterior telopods indistinctly demarcated from each other only in anterior views..... *S. aesculus* Rosenmejer & Wesener, 2021

Discussion

This study integrates morphological and COI barcode data to describe new species of the giant pill-millipede genus *Sphaerobelum* from Thailand and Laos. The three new species clearly belong to the species group characterised by a superficially unmodified (but apically mini-toothed) mesal margin of the leg femur. They share distinct morphological traits typical of the genus, such as the hammer-shaped process of telopoditomere 2 of the posterior telopods. However, they can be differentiated from all other known congeners by a combination of characters, including body colour, spines on tarsal legs, a row of bristles on the endotergum, the vulva shape, and details of the telopods (Wesener 2016; Semenyuk et al. 2018). Molecular analyses of COI sequences further support the designation of these specimens as new species.

While most *Sphaerobelum* species are brown, eight species, including the two newly described species herein, *S. nonghinensis* sp. nov. and *S. onyx* sp. nov., exhibit a striking black and shiny appearance (Fig. 16), alongside six previously known species (*S. bicorne*, *S. denticulatum* Wesener, 2019, *S. laoticum*, *S. nigrum* Wesener, 2019, *S. pumatense* Semenyuk, Golovatch & Wesener, 2020, *S. schwendingeri*). Such unique colour features endow the giant pill millipede with a distinctive, exotic appearance that often attracts the attention of collectors.

The genetic distances of three new species compared to their congeners are relatively high: 13.24–22.12% for *S. nonghinensis* sp. nov., 13.24–20.85% for *S. onyx* sp. nov., and 13.85–21.22% for *S. petramurum* sp. nov.

These values fall within the typical range of interspecific *p*-distances for most giant pill millipede genera, such as the *Zephronia* and *Prionobelum*, which are between 8% and 21% (Rosenmejer et al. 2021; Bhansali and Wesener 2022; Donworth and Wesener 2024; Srisonchai et al. 2024b). Notably, high intraspecific genetic distances of COI fragments (658 base pairs) are also observed in *S. onyx* sp. nov. and S. *petramurum* sp. nov. In the case of *S. onyx* sp. nov., the genetic divergence of the Thai population reaches 5.02% when compared to the Laotian specimen from Vang Vieng. For *S. petramurum* sp. nov., the *p*-distance between populations from its type locality in Phu Pha Man District and those from Khon Sarn District ranges from 0 to 7.15%. This divergence may be attributed to geographical separations of approximately 200 km for *S. onyx* sp. nov. and 50 km for *S. petramurum* sp. nov., indicating a pattern of isolation by distance, similar to trends seen in other giant pill-millipede genera and across different millipede orders (Wesener et al. 2014; Means and Marek 2017; Bhansali and Wesener 2022; Srisonchai et al. 2024b). *Sphaerobelum petramurum* sp. nov. specifically inhabits limestone environments scattered throughout the Phetchabun mountain range, with each population confined to distinct limestone karst formations.

The low genetic distance observed between the genera *Zephronia* and *Sphaerobelum* is the result of the minimal genetic divergence between the species *S. benqii* Liu & Wesener, 2022, and *Zephronia hui* Liu & Wesener, 2022. These two species exhibit an interspecific genetic divergence of only 6.8% (see Zhao et al. 2022), which is comparable to intraspecific divergence levels within species of the family Zephroniidae. Morphologically, however, *S. benqii* is more closely related to the morphologically distinct Thai species of *Sphaerobelum*, namely *S. aesculus* and *S. meridionalis*, with which it clusters in our maximum likelihood (ML) analysis (Fig. 1). The genetic position of *Zephronia hui* based on the COI gene is an anomaly, as its morphology unequivocally places it within the genus *Zephronia* (Zhao et al. 2022). This low divergence between the two species may result from relying solely on a single mitochondrial marker, the COI gene, which may not fully capture the extent of genetic variation.

A key aspect of using DNA-based approaches for species delimitation is their ability to distinguish species boundaries (Filgueiras et al. 2011; Li and Li 2018; Srisonchai et al. 2024a; Twomey et al. 2023). The molecular and morphological evidence presented in this study strongly supports the identification of the three distinct monophyletic clades as new species within the *Sphaerobelum*. Our results also provide some insight into the relationships among certain species, though this aspect is beyond the scope of our study and at least highlight that most *Sphaerobelum* species cluster within the same major clade (Fig. 1). However, preliminary phylogenetic trees based on a single gene fragment remain unclear, raising questions about the interrelationships among the most *Sphaerobelum* species and their related genera (*Zephronia*, *Prionobelum*, and *Cryxus*). To improve our understanding of these relationships, further research is needed to gather additional genetic data from more taxa, particularly the type species, *S. clavigerum*, and to incorporate a broader range of genetic markers (Means and Marek 2017, 2021a, 2021b; Hennen et al. 2022).

The three new species are geographically separated from one another, and all are currently found in limited areas. Of these, *S. onyx* sp. nov. has a wider distribution near the Thai-Laos border along the Mekong River, while the other two species, *S. nonghinensis* sp. nov. and *S. petramurum* sp. nov., are restricted to limestone habitats in the Phetchabun mountain range.

Intensive field surveys in the northeastern region have led to the discovery of three new species, bringing the total number of *Sphaerobelum* species in Thailand to seven (with 27 valid species worldwide). Our findings highlight the significant hidden biodiversity of millipedes, particularly in the unexplored limestone areas and sandstone of the region (Foon et al. 2017; Srisonchai et al. 2018a, 2018b; Grismer et al. 2020; Tolentino et al. 2020). We firmly believe that more new giant millipede species will be uncovered with further investigations.

Acknowledgements

Thanks are due to all curators and staff, including Henrik Enghoff (NHMD), Nesrine Akkari and Oliver Macek (NHMW), Jason Dunlop and Anja Friederichs (ZMB), for access to and loan of the type materials. Department of National Parks, Wildlife and Plant Conservation, Thailand, provided permission to conduct the research in restricted areas. Thanks are further due to our colleagues of the Animal Systematic Research Unit (ASRU) in the Department of Biology, Faculty of Science, Chulalongkorn University, and MZKKU students at the Department of Biology, Faculty of Science, Khon Kaen University, for fieldwork assistance. Special thanks go to P. Sukkharom for providing specimens of *S. turcosa* and D. J. Anderson for English corrections. The editor (Luiz F. M. Iniesta) and reviewers (Sergei I. Golovatch and Piyatida Pimvichai) are acknowledged for their useful comments, which have improved the quality of the manuscript. The ZSE copy editor and staff (Bilyana Nikolova and Joel Akumiah) carefully edited the final version of the manuscript. The CIPRES Science Gateway allowed the computational analyses.

This work was funded by the National Science, Research and Innovation Fund of Khon Kaen University (2567) and partly supported by the Office of the Permanent Secretary, Ministry of Higher Education, Science, Research and Innovation (OPS MHESI), Thailand Science Research and Innovation (TSRI) (Grant No. RGNS65-056). The research capability enhancement program through graduate student scholarship (KS), Faculty of Science, Khon Kaen University, is gratefully acknowledged.

References

American Veterinary Medical Association (2020) AVMA Guidelines for the euthanasia of animals: 2020 Edition. American Veterinary Medical Association, United States.

Attems C (1938) Die von Dr. C. Dawydoff in französisch Indochina gesammelten Myriopoden. Mémoires du Muséum National d'Histoire Naturelle 6(2): 187–353.

Attems C (1953) Myriopoden von Indochina, Expedition von Dr. C Dawydoff (1938–1939). Mémoires du Muséum National d'Histoire Naturelle (n.s., A)5: 133–230.

Bhansali S, Wesener T (2022) New Thai Giant Pill-Millipede species, with genetic barcoding data for Thai species (Diplopoda, Sphaerotheriida, Zephroniidae). Zootaxa 5105(3): 357–380. https://doi.org/10.11646/zootaxa.5105.3.2

Clements R, Sodhi NS, Schilthuizen M, Ng PKL (2006) Limestone karsts of Southeast Asia: Imperiled arks of biodiversity. BioScience 56: 733–742. https://doi.org/10.1641/0006-3568(2006)56[733:LKOSAI]2.0.CO;2

Clements R, Ng PKL, Lu XX, Ambu S, Schilthuizen M, Bradshaw CJA (2008) Using biogeographical patterns of endemic land snails to improve conservation planning for limestone karsts. Biological Conservation 141(11): 2751–2764. https://doi.org/10.1016/j.biocon.2008.08.011

Donworth P, Wesener T (2024) The first record of the giant pill-millipede genus *Prionobelum* Verhoeff, 1924 from Thailand, with the integrative description of two species (Diplopoda, Sphaerotheriida, Zephroniidae). Zootaxa 5419(4): 545–562. https://doi.org/10.11646/zootaxa.5419.4.4

Filgueiras BKC, Lannuzzi L, Leal IR (2011) Habitat fragmentation alters the structure of dung beetle communities in the Atlantic Forest. Biological Conservation 144(1): 362–369. https://doi.org/10.1016/j.biocon.2010.09.013

Folmer O, Black M, Hoeh W, Lutz R, Vrijenhoek R (1994) DNA primers for amplification of mitochondrial cytochrome c oxidase subunit I from diverse metazoan invertebrates. Molecular Marine Biology and Biotechnology 3: 294–299.

Foon JK, Clements GR, Liew T-S (2017) Diversity and biogeography of land snails (Mollusca, Gastropoda) in the limestone hills of Perak, Peninsular Malaysia. ZooKeys 682: 1–94. https://doi.org/10.3897/zookeys.682.12999

Furukawa H, Pichai W (1989) Salt and sinkhole: Corrosion as a principal factor governing topography and mass movement in Northeast Thailand. Southeast Asian Studies 27(1): 3–34. https://doi.org/10.20495/tak.27.1_3

Grismer LL, Wood PL, Le MD, Quah ESH, Grismer JL (2020) Evolution of habitat preference in 243 species of Bent-toed geckos (Genus *Cyrtodactylus* Gray, 1827) with a discussion of karst habitat conservation. Ecology and Evolution 10: 13717–13730. https://doi.org/10.1002/ece3.6961

Hennen DA, Means JC, Marek PE (2022) A revision of the *wilsoni* species group in the millipede genus *Nannaria* Chamberlin, 1918 (Diplopoda, Polydesmida, Xystodesmidae). ZooKeys 1096: 17–118. https://doi.org/10.3897/zookeys.1096.73485

Huelsenbeck JP, Hillis DM (1993) Success of phylogenetic methods in the four-taxon case. Systematic Biology 42: 247–264. https://doi.org/10.1093/sysbio/42.3.247

Jeekel CAW (1971) Nomenclator generum et familiarum Diplopodorum: A list of the genus and family-group names in the Class Diplopoda from the 10th edn of Linnaeus, 1758, to the end of 1957. Monografieen van de Nederlandse Entomologische Vereniging 5: 1–412.

Joint Publications Research Service Arlington VA (1965) Geographical index of Thailand. First Edition. Joint Publications Research Service Arlington VA, United States.

Kalyaanamoorthy S, Minh BQ, Wong TKF, von Haeseler A, Jermiin LS (2017) ModelFinder: fast model selection for accurate phylogenetic estimates. Nature Methods 14: 587–589. https://doi.org/10.1038/nmeth.4285

Larget B, Simon DL (1999) Markov Chain Monte Carlo algorithms for the Bayesian analysis of phylogenetic trees. Molecular Biology and Evolution 16: 750–759. https://doi.org/10.1093/oxfordjournals.molbev.a026160

Li F, Li S (2018) Paleocene-Eocene and Plio-Pleistocene sea-level changes as "species pumps" in Southeast Asia: Evidence from *Althepus* spiders. Molecular Phylogenetics and Evolution 127(2018): 545–555. https://doi.org/10.1016/j.ympev.2018.05.014

Likhitrakarn N, Srisonchai R, Golovatch SI (2023) An updated catalogue of the millipedes (Diplopoda) of Thailand. Tropical Natural History, Supplement 7: 51–92. https://li01.tci-thaijo.org/index.php/tnh/article/view/258815

Means JC, Marek PE (2017) Is geography an accurate predictor of evolutionary history in the millipede family Xystodesmidae? PeerJ 5: e3854. https://doi.org/10.7717/peerj.3854

Means JC, Hennen DA, Marek PE (2021a) A revision of the minor species group in the millipede genus *Nannaria* Chamberlin, 1918 (Diplopoda, Polydesmida, Xystodesmidae). ZooKeys 1030: 1–180. https://doi.org/10.3897/zookeys.1030.62544

Means JC, Hennen DA, Tanabe T, Marek PE (2021b) Phylogenetic systematics of the millipede family Xystodesmidae. Insect Systematics and Diversity 5(2): 1–12. https://doi.org/10.1093/isd/ixab003

Miller MA, Pfeiffer W, Schwartz T (2010) Creating the CIPRES Science Gateway for inference of large phylogenetic trees. In: 'Proceedings of the Gateway Computing Environments Workshop (GCE)', 14 November 2010, New Orleans, LA, USA. INSPEC Accession Number: 11705685, 1–8. https://doi.org/10.1109/GCE.2010.5676129

Minh BQ, Schmidt HA, Chernomor O, Schrempf D, Woodhams MD, von Haeseler A, Lanfear R (2020) IQ-TREE 2: New models and efficient methods for phylogenetic inference in the genomic era. Molecular Biology and Evolution 37: 1530–1534. https://doi.org/10.1093/molbev/msaa015

Pholyotha A, Sutcharit C, Tongkerd P, Panha S (2020) Integrative taxonomic revision of the land snail genus *Sarika* Godwin-Austen, 1907 in Thailand, with descriptions of nine new species (Eupulmonata, Ariophantidae). ZooKeys 976: 1–100. https://doi.org/10.3897/zookeys.976.53859

Pimvichai P, Enghoff H, Panha S, Backeljau T (2020) Integrative taxonomy of the new millipede genus *Coxobolellus*, gen. nov. (Diplopoda, Spirobolida, Pseudospirobolellidae), with descriptions of ten new species. Invertebrate Systematics 34(6): 591–617. https://doi.org/10.1071/IS20031

Plant AR (2014) Areas of endemism in Thailand: has historical partitioning between seasonally dry lowland and a seasonal moist mountain forests shaped biodiversity in Southeast Asia? Raffles Bulletin of Zoology 62: 812–821.

Prueksapong A, Watanabe T, Funakawa S (2015) Profile description, properties, and classification of paddy soils at different topographical positions in Surin Province, Thailand. Japan Science and Technology Agency 59(2): 63–73. https://doi.org/10.18920/pedologist.59.2_63

Rambaut A (2018) Figtree ver 1.4.4. Institute of Evolutionary Biology, University of Edinburgh, Edinburgh. http://tree.bio.rd.ac.uk/software/figtree/ [16 January 2023, data last accessed]

Ronquist F, Teslenko M, van der Mark P, Ayres DL, Darling A, Höhna S, Larget B, Liu L, Suchard MA, Huelsenbeck JP (2012) MrBayes 3.2: Efficient Bayesian phylogenetic inference and model choice across a large model space. Systematic Biology 61: 539–542. https://doi.org/10.1093/sysbio/sys029

Rosenmejer T, Enghoff H, Moritz L, Wesener T (2021) Integrative description of new giant pill-millipedes from southern Thailand (Diplopoda, Sphaerotheriida, Zephroniidae). European Journal of Taxonomy 762: 108–132. https://doi.org/10.5852/ejt.2021.762.1457

Semenyuk I, Golovatch SI, Wesener T (2018) Four new species of giant pill-millipedes from Vietnam (Sphaerotheriida, Zephroniidae). Zootaxa 4459(3): 535–550. https://doi.org/10.11646/zootaxa.4459.3.7

Semenyuk I, Golovatch SI, Wesener T (2020) Some new or poorly-known Zephroniidae (Diplopoda, Sphaerotheriida) from Vietnam. ZooKeys 930: 37–60. https://doi.org/10.3897/zookeys.930.47742

Srisonchai R, Enghoff H, Likhitrakarn N, Panha S (2018a) A revision of dragon millipedes I: genus *Desmoxytes* Chamberlin, 1923, with the description of eight new species (Diplopoda, Polydesmida, Paradoxosomatidae). ZooKeys 761: 1–177. https://doi.org/10.3897/zookeys.761.24214

Srisonchai R, Enghoff H, Likhitrakarn N, Panha S (2018b) A revision of dragon millipedes II: the new genus *Nagaxytes* gen. nov., with the description of three new species (Diplopoda, Polydesmida, Paradoxosomatidae). European Journal of Taxonomy 463: 1–43. https://doi.org/10.5852/ejt.2018.462

Srisonchai R, Likhitrakarn N, Sutcharit C, Backeljau T, Pimvichai P (2023) A new jewel-like species of the pill-millipede genus *Sphaerobelum* Verhoeff, 1924 (Diplopoda, Sphaerotheriida, Zephroniidae) from Thailand. ZooKeys 1181: 41–57. https://doi.org/10.3897/zookeys.1181.109076

Srisonchai R, Enghoff H, Likhitrakarn N, Jeratthitikul E, Jirapatrasilp P, Panha S, Sutcharit S (2024a) Molecular phylogeny of dragon millipedes (Diplopoda, Polydesmida, Paradoxosomatidae) from mainland South-East Asia, with description of a new genus and species. Zoological Journal of the Linnean Society 202(11): zlad164. https://doi.org/10.1093/zoolinnean/zlad164

Srisonchai R, Likhitrakarn N, Sutcharit C, Wesener T (2024b) Integrative taxonomy reveals two new giant pill-millipedes of the genus *Zephronia* Gray, 1832 from eastern Thailand (Diplopoda, Sphaerotheriida, Zephroniidae). ZooKeys 1212: 29–64. https://doi.org/10.3897/zookeys.1212.126536

Tamura K, Stecher G, Kumar S (2021) MEGA11: Molecular Evolutionary Genetics Analysis version 11. Molecular Biology and Evolution 38: 3022–3027. https://doi.org/10.1093/molbev/msab120

Tanabe AS (2011) Kakusan4 and Aminosan: two programs for comparing nonpartitioned, proportional and separate models for combined molecular phylogenetic analyses of multilocus sequence data. Molecular Ecology Resources 11: 914–921. https://doi.org/10.1111/j.1755-0998.2011.03021.x

Tolentino PJ, Navidad JRL, Aangeles MD, Fernandez DAP, Villanueva ELC, Obeña RDR, Buot IEJr (2020) Biodiversity of forests over limestone in Southeast Asia with emphasis on the Philippines. Biodiversitas 21(4): 1597–1613. https://doi.org/10.13057/biodiv/d210441

Twomey E, Melo-Sampaio P, Schulte LM, Bossuyt F, Brown JL, Castroviejo-Fisher S (2023) Multiple routes to color convergence in a radiation of neotropical poison frogs. Systematic Biology 72(6): 1247–1261. https://doi.org/10.1093/sysbio/syad051

Verhoeff KW (1924) Results of Dr. E. Mjöberg's Swedish scientific expedition to Australia 1910–1913. 34. Myriapoda: Diplopoda. Arkif för Zoologi 16(5): 1–142.

Wesener T (2016) The giant pill-millipedes, order Sphaerotheriida – An annotated species catalogue with morphological atlas and list of apomorphies (Arthropoda, Diplopoda). Bonn Zoological Bulletin Supplementum 63: 1–104.

Wesener T (2019) First records of giant pill-millipedes from Laos (Diplopoda, Sphaerotheriida, Zephroniidae). Zootaxa 4563(2): 201–248. https://doi.org/10.11646/zootaxa.4563.2.1

Wesener T, VandenSpiegel D (2009) A first phylogenetic analysis of Giant Pill-Millipedes (Diplopoda, Sphaerotheriida), a new model Gondwanan taxon, with special emphasis on island gigantism. Cladistics 25: 545–573. https://doi.org/10.1111/j.1096-0031.2009.00267.x

Wesener T, Raupach MJ, Sierwald P (2010) The origins of the giant pill-millipedes from Madagascar (Diplopoda, Sphaerotheriida, Arthrosphaeridae). Molecular phylogenetics and evolution 57(3): 1184–1193. https://doi.org/10.1016/j.ympev.2010.08.023

Wesener T, Le D, Loria S (2014) Integrative revision of the giant pill-millipede genus *Sphaeromimus* from Madagascar, with the description of seven new species (Diplopoda, Sphaerotheriida, Arthrosphaeridae). ZooKeys 414: 67–107. https://doi.org/10.3897/zookeys.414.7730

Willett W, Jenny B, Isenberg T, Dragicevic P (2015). Lightweight relief shearing for enhanced terrain perception on interactive maps. Proceedings of the 33rd ACM Conference on Human Factors in Computing Systems (CHI 2015), Apr 2015, Seoul, South Korea, 3563–3572. https://doi.org/10.1145/2702123.2702172

Wongthamwanich N, Panha S, Sierwald P, Wesener T, Thirakhupt K (2012) A new species of the giant pill-millipede genus *Sphaerobelum* Verhoeff, 1924 from northern Thailand, with an extensive description and molecular characters (Diplopoda, Sphaerotheriida, Zephroniidae). Zootaxa 3220: 29–43. https://doi.org/10.11646/zootaxa.3220.1.2

Zhao Y, Yu J, Liu W (2020) A molecular-based phylogeny of the millipede genus *Sphaerobelum* Verhoeff, 1924, with the first record of the genus from mainland China (Diplopoda, Sphaerotheriida, Zephroniidae). Annales de la Société Entomologique de France (N.S.) 56: 341–348. https://doi.org/10.1080/00379271.2020.1811153

Zhao Y, Hu L, Wesener T, Liu W (2022) Five new species of the giant pill-millipedes of the genera *Zephronia* and *Sphaerobelum*, from China (Diplopoda: Sphaerotheriida: Zephroniidae). Annales de la Société Entomologique de France 58: 499–524. https://doi.org/10.1080/00379271.2022.2137059

Supplementary material 1

List of species with GenBank accession numbers of COI gene used in this study

Authors: Khanet Srikampha, Thomas Wesener, Natdanai Likhitrakarn, Chirasak Sutcharit, Ruttapon Srisonchai

Data type: docx

Copyright notice: This dataset is made available under the Open Database License (http://opendatacommons.org/licenses/odbl/1.0/). The Open Database License (ODbL) is a license agreement intended to allow users to freely share, modify, and use this Dataset while maintaining this same freedom for others, provided that the original source and author(s) are credited.

Link: https://doi.org/10.3897/zse.101.143073.suppl1

Supplementary material 2

Genetic divergences of cytochrome c oxidase I (COI) sequence (uncorrected p-distances) within and among *Sphaerobelum* species and related genera

Authors: Khanet Srikampha, Thomas Wesener, Natdanai Likhitrakarn, Chirasak Sutcharit, Ruttapon Srisonchai

Data type: xlsx

Copyright notice: This dataset is made available under the Open Database License (http://opendatacommons.org/licenses/odbl/1.0/). The Open Database License (ODbL) is a license agreement intended to allow users to freely share, modify, and use this Dataset while maintaining this same freedom for others, provided that the original source and author(s) are credited.

Link: https://doi.org/10.3897/zse.101.143073.suppl2